

TABLE 1
OBSERVED AND DERIVED CO PROPERTIES

HCG ^a	Type ^b	R ₂₅ ^c "	Beam "	v_{opt} ^d km/s	v_{CO} ^e km/s	T_{mb} ^f mK	Δv_{CO} ^g km/s	I_{CO} ^h Kkm/s	M_{H_2} $10^8 M_{\odot}$	$\log(L_B)$ L_{\odot}	Other names
7b	SB0	40.1	55	4238	<0.7	<7.3	10.18	N196
7c	SBc	52.3	55	4366	4422	18.1	183	1.4	15.0	10.65	N201
10a	SBb	104.8	55	5148	<0.9	<10.7	10.79	N536
10b	E1	51.2	55	4862	<0.9	<12.5	10.72	N529
10c	Sc	55.4	55	4660	<0.9	<12.1	10.12	N531
10d	Scd	29.2	55	4620	<1.6	<22.0	9.86	N542
18b	S/Irr	50.0	55	4082	4059	7.3	42	0.6	6.2	9.66	U2140a
18c	Im	22.8	55	4143	<0.3	<3.1	9.39	U2140b
21a	Sc	44.8	55	7614	7618	15.2	555	4.8	165.6	10.53	...
21b	Sab	45.9	55	7568	<0.6	<21.8	10.65	...
21c	E1	29.2	55	7356	<0.8	<26.6	10.54	...
21d	E2	18.0	55	8835	<0.8	<29.0	10.27	...
21e	SB0a	17.4	55	8843	<0.9	<30.8	10.02	...
22a	E2	79.8	55	2705	<0.7	<3.0	10.38	N1199
22b	Sa	30.6	55	2625	<0.8	<3.6	9.46	...
22c	SBcd	52.3	55	2728	<1.0	<4.0	9.71	...
30a	SBa	55.5	55	4697	<0.7	<9.2	10.62	...
30b	Sa	36.5	55	4625	<0.7	<9.1	10.29	...
30c	SBbc	17.3	55	4508	<0.8	<9.7	9.69	...
30d	S0	15.4	55	4666	<0.8	<10.9	9.49	...
31a	Sdm	32.3	55	4042	3999 ⁱ	8.0 ⁱ	168 ⁱ	0.4 ^j	4.4 ^j	9.69	N1741
31c	Im	18.3	55	4068	10.62	M1089
31b ^j	Sm	26.1	55	4171	<0.7	<7.2	9.92	...
31g ^k	Irr	18.0	55	4012	<0.4	<4.1	9.73	M1090
33a	E1	11.1	55	7570	<0.5	<17.1	10.05	...
33c	Sd	23.3	55	7823	7809	7.9	196	1.0	38.2	9.64	...
35a	S0	14.4	55	15919	<0.3	< 43.5	9.75	...
35d	Sc	11.6	55	15798	<0.3	< 51.6	9.22	...
35f	E1	4.1	55	16330	<0.3	< 51.6	8.79	...
38a	Sbc	22.1	55	8760	8662	9.8	362	1.4	67.3	10.21	...
38b	SBd	30.0	55	8739	8691 ⁱ	9.6 ⁱ	258 ⁱ	1.4 ⁱ	66.4 ⁱ	10.39	U5044a
38c	Im	21.8	55	8770	10.10	U5044b
44a	Sa	100.7	18	1293	<20.7	<2.6	10.02	N3190
44c	E2	56.8	18	1218	<16.5	<2.0	9.55	N3185
48a	E2	45.7	55	3014	<1.0	<4.8	9.84	I2597
48b	Sc	22.0	55	2385	<1.2	<5.9	9.32	...
48c	S0a	15.4	55	4203	4266	13.5	329	1.6	7.7	9.38	...
48d	E1	8.8	55	3045	2969	12.1	111	0.9	4.1	8.71	...
59a	Sa	17.7	55	4109	4122	14.9	57	1.0	10.2	9.84	I736
59b	E0	15.0	55	3908	<0.9	<8.8	9.52	...
59c	Sc	24.7	55	4347	<0.7	<7.2	9.92	...
59d	Im	17.7	55	3866	<0.7	<6.6	9.25	I737
61a	E/S0	54.3	30	3784	3683	12.9	84	0.6	1.7	10.45	N4169
61c	Sbc	51.8	30	3956	3950	39.4	561	10.3	28.2	10.19	N4175
61d	S0	25.6	30	3980	<0.7	<1.9	9.97	N4174

TABLE 1—*Continued*

HCG ^a	Type ^b	R ₂₅ ^c "	Beam "	v_{opt} ^d km/s	v_{CO} ^e km/s	T_{mb} ^f mK	Δv_{CO} ^g km/s	I _{CO} ^h Kkm/s	M _{H₂} 10 ⁸ M _⊙	log(L _B) L _⊙	Other names
67a	E1	58.8	55	7262	<0.9	<28.0	11.07	...
67b	Sc	68.4	55	7644	7625	8.8	234	2.3	75.3	10.63	...
67c	Scd	19.9	55	7430	<0.8	<25.6	10.13	...
68a	S0	77.4	55	2162	1840	18.1	485	2.1	7.4	10.40	N5353
68b	E2	86.4	55	2635	<0.7	<2.1	10.36	N5354
68c	SBbc	76.7	55	2313	2336	25.2	327	5.1	17.8	10.36	N5350
68d	E3	31.1	55	2408	2535	11.1	50	0.3	1.2	9.68	N5355
69a	Sc	47.5	55	8856	<0.7	<30.8	10.34	U8842
69b	SBb	14.8	55	8707	<0.6	<34.1	10.07	...
69c	S0	13.4	55	8546	<0.7	<26.6	10.34	U8842
69d	SB0	10.8	55	9149	<0.7	<30.8	9.95	U8842
79b	S0	60.5	55	4446	<0.5	<5.8	10.21	N6027
79c	S0	40.3	55	4146	<0.5	<5.8	9.77	N6027
85a	E1	16.0	55	11155	<0.3	<26.3	8.48	...
85b	E1	13.1	55	12122	<0.3	<24.6	8.81	...
88b	SBb	34.0	55	6010	<0.8	<17.9	10.68	N7977
88c	Sc	27.6	55	6083	5952	17.6	251	2.0	44.3	10.43	N6976
88d	Sc	32.7	55	6032	<1.0	<21.7	10.18	N6975
90a	Sa	71.8	55	2575	2495	18.1	586	6.0	25.7	10.29	N7172
90b	E0	39.9	55	2525	2762 ⁱ	18.3 ⁱ	618 ⁱ	5.8 ⁱ	24.8 ⁱ	10.19	N7176
90d	Im	69.3	55	2778	10.16	N7174
90c	E0	36.6	55	2696	2651	19.2	18	0.7	3.0	10.12	N7173
92a	Sd	69.8	55	786	780	20.7	22	0.3	0.1	9.17	N7320
92b	Sbc	66.6	55	5774	<0.5	<12.6	10.66	N7318B
92c	SBc	52.8	55	6764	6657	6.1	195	0.6	15.1	10.74	N7319
92d	Sc	36.6	55	6630	<0.5	<15.1	10.60	N7318A
95a	E3	26.3	55	11888	<0.4	<30.1	10.86	N7609
95b	Scd	20.7	55	11637	<0.3	<25.8	10.42	...
95c	Sm	28.4	55	11562	<0.4	<30.1	10.46	...
95d	Sc	22.1	55	12350	<0.4	<31.0	10.16	...
96a	SBc	33.3	55	8670	8664	31.8	251	5.1	239.9	10.90	N7674
96b	E2	18.7	55	8585	<0.3	<14.1	10.53	N7675
96c	Sa	12.2	55	8805	8912	5.7	92	0.4	18.6	10.05	...
96d	Sm	6.6	55	9025	<0.8	<37.2	9.69	...
I 883	S+S	46.5	55	6892	6996	26.8	476	7.2	208.4	10.40	...
N 2738	S?	43.4	55	3065	3120	33.3	230	3.4	19.5	10.07	...
N 6090	S+S	50.9	55	8785	8824	41.7	130	4.3	202.1
Data from bibliography											
7a ^l	Sb	56.8	43	4210	4168	...	500	7.2	49.2	10.47	N192
7d ^l	SBc	38.3	43	4116	<0.6	<2.5	9.73	N197
16a ^l	SBab	34.9	43	4152	4061	...	370	8.7	51.3	10.55	N835
16b ^l	Sab	49.4	43	3977	3786	...	560	2.3	13.5	10.30	N833
16c ^l	Im	31.5	43	3861	3829	...	270	9.2	53.7	10.34	N838
16d ^l	Im	41.1	43	3847	3846	...	240	6.5	38.0	10.21	N839
37a ^l	E7	51.9	23	6745	<1.4	<6.6	10.91	N2783
44d ⁿ	Sd	67.7	23	1579	1550	40	60	3.0	0.6	9.56	N3187

TABLE 1—*Continued*

HCG ^a	Type ^b	R ₂₅ ^c "	Beam "	v_{opt} ^d km/s	v_{CO} ^e km/s	T_{mb} ^f mK	Δv_{CO} ^g km/s	I_{CO} ^h Kkm/s	M_{H_2} $10^8 M_\odot$	$\log(L_B)$ L_\odot	Other names
87a ¹	Sbc	39.8	43	8694	<0.5	<14.8	10.71	...
88a ¹	Sb	45.1	43	6033	1.2	16.2	10.71	N6978

^aNotation as in Hickson et al. (1992).

^bMorphological types from Mendes de Oliveira & Hickson (1994) and Williams & Rood (1987). In the case of H61a, although classified by Mendes de Oliveira & Hickson (1994) as S0a, Rubin et al (1991) indicate that it is an elliptical galaxy, according to its light profile.

^cRadius in arcseconds of the $\mu_B = 25.0$ mag arcsec⁻² isophote from Hickson (1993).

^dOptical velocities from Hickson (1993), except for H18b from Williams & Van Gorkom (1988), and H96 from our optical spectroscopy data (Verdes-Montenegro et al. 1996).

^eIntensity weighted velocity in the range for which the line has been detected.

^fPeak line main beam brightness temperature in units of mK.

^gFull width of the CO line measured at a 30% of the peak line temperature given in column 6, except for galaxies from Boselli et al. (1996) for which the corresponding level is not given.

^hGiven fluxes are already corrected for extended sources as explained in §2.3. Upper limits for non-detection have been calculated by taking the 3σ rms noise multiplied by an assumed line width of 300 km/s and divided by the square root of number of channels in that velocity range.

ⁱThe emission is unresolved. Therefore we give parameters for the global profile.

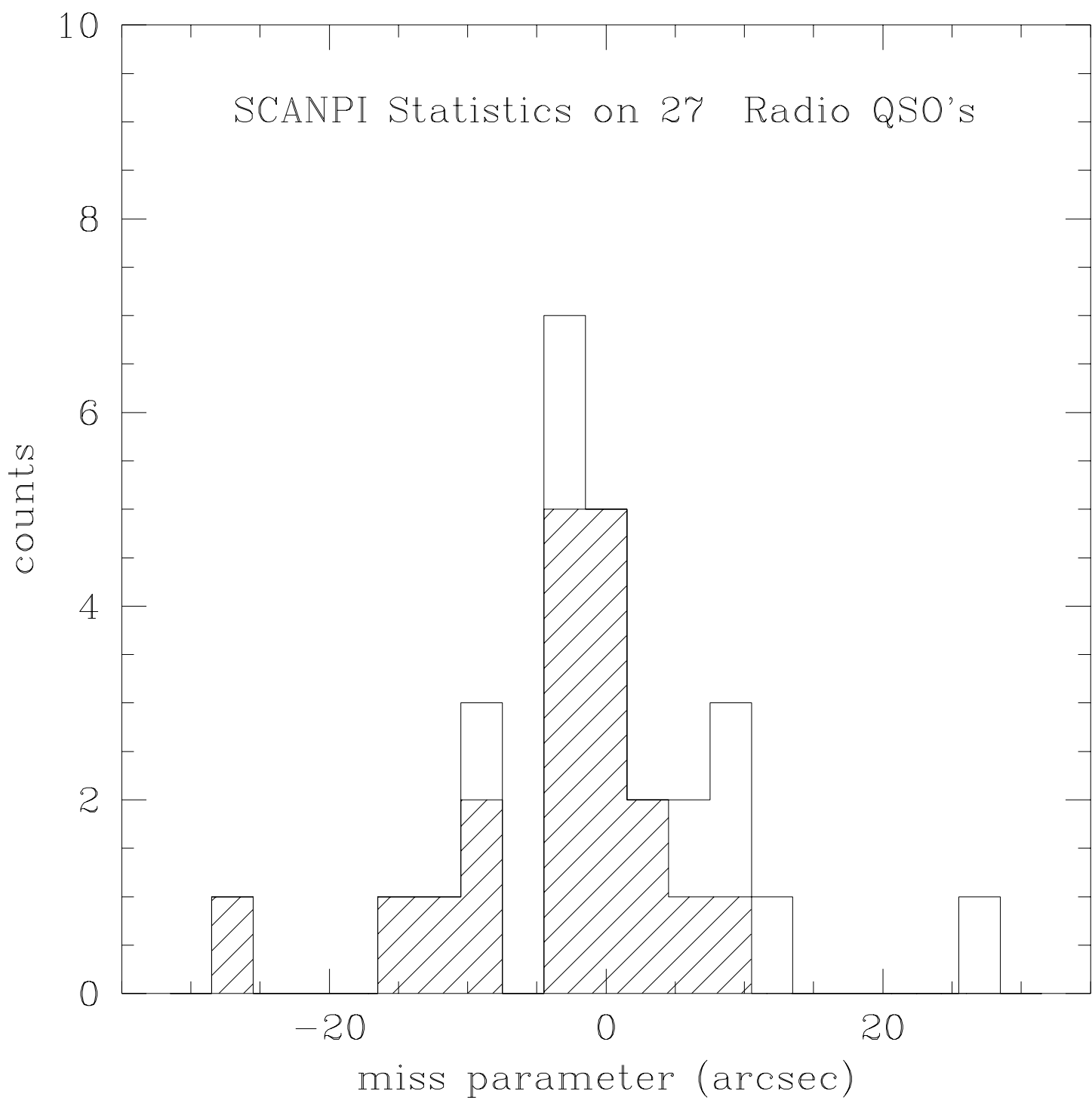
^jThe upper limits is from Kitt Peak observations, and the lower one from OVRO measurement (Yun et al 1997) sensible to the more compact emission.

^kThis member has been added to H31 by Rubin, Hunter, & Ford (1990).

¹Data from Boselli et al. (1996).

^mData from Wilklind et al. (1995).

ⁿData from Braine & Combes (1993).



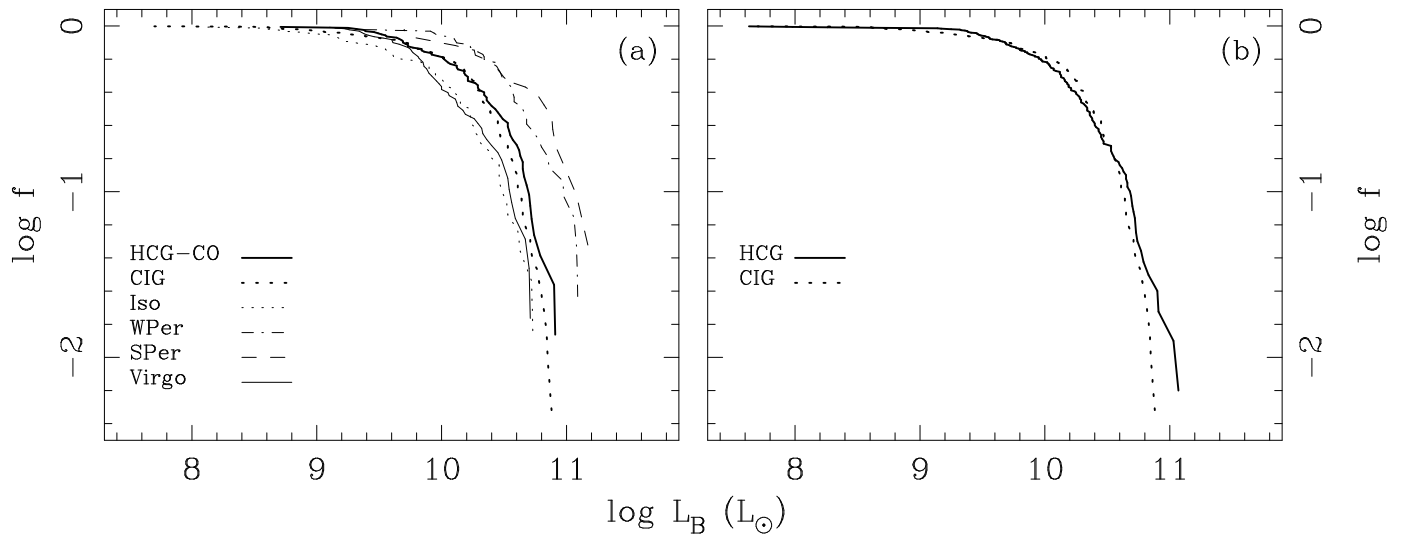


TABLE 2
FIR PARAMETERS OF OUR SAMPLE OF HCG GALAXIES

HCG	I ₁₂ (Jy)	I ₂₅ (Jy)	I ₆₀ (Jy)	I ₁₀₀ (Jy)	L _{FIR} (L _⊙)	HCG	I ₁₂ (Jy)	I ₂₅ (Jy)	I ₆₀ (Jy)	I ₁₀₀ (Jy)	L _{FIR} (L _⊙)
3a	<0.132	<0.141	0.240	<0.336	<9.558	38a	<0.069	<0.189	0.440	1.200	10.105
3b	<0.099	<0.114	<0.176	<0.528	<9.634	38bc	0.100	0.270	1.600	3.370	10.611
3c	<0.126	<0.147	0.640	1.200	10.433	38d	<0.102	0.180	0.190	<0.600	<10.670
3d	<0.111	<0.120	0.150	<0.384	<9.523	40a	<0.060	<0.084	<0.099	<0.300	<9.238
4a	0.300	0.650	4.230	8.880	10.957	40b	<0.057	<0.093	<0.084	<0.255	<9.905
4b	<0.117	<0.105	0.400	<0.300	<9.673	40c	0.090	0.110	0.850	2.000	10.149
4c	<0.056	<0.108	<0.090	<0.306	<9.478	40d	<0.072	0.100	1.030	2.300	10.170
4d	<0.111	<0.114	<0.117	<0.297	<9.458	40e	<0.066	<0.090	<0.099	<0.240	<9.188
4e	<0.093	<0.111	<0.087	<0.351	<10.152	42					IRAS GAP
7a	0.230	0.370	3.320	6.610	10.278	44a	0.350	0.460	3.400	10.72	9.359
7b	<0.099	<0.225	<0.183	<0.318	<9.001	44b	<0.084	<0.129	<0.123	<0.390	<7.975
7c	0.180	0.310	0.610	2.350	9.722	44c	0.210	0.280	1.550	3.710	8.905
7d	<0.114	<0.210	<0.153	<0.390	<8.972	44d	<0.099	0.240	1.300	3.120	9.055
10a	<0.069	0.120	0.500	1.810	9.764	46a	<0.060	<0.204	<0.066	<0.210	<9.259
10b	<0.075	<0.078	<0.108	0.470	<9.097	46b	<0.081	<0.120	<0.066	<0.210	<9.298
10c	0.090	<0.201	0.780	2.060	9.795	46c	<0.081	<0.114	<0.090	<0.219	<9.301
10d	<0.084	<0.108	<0.120	<0.276	<8.946	46d	<0.090	<0.123	<0.075	<0.219	<9.240
16a	0.350	0.400	5.730	12.830	10.526	48a	0.430	<0.111	<0.102	<0.429	<8.398
16b	<0.06	<0.100	<0.120	<0.330	<8.822	48b	0.160	0.320	0.960	2.150	9.286
16c	1.100	2.060	12.200	19.990	10.731	48c	<0.066	<0.102	<0.090	<0.183	<8.748
16d	0.500	2.400	11.800	12.000	10.646	48d	<0.057	<0.084	<0.093	<0.141	<8.404
18a	<0.108	<0.117	<0.108	<0.300	<9.617	51					IRAS GAP
18b	<0.090	<0.096	<0.129	<0.357	<8.909	54 ^a	<0.051	0.240	0.500	0.840	8.465
18c	<0.096	<0.117	<0.105	<0.357	<8.881	56a	<0.060	<0.069	<0.111	<0.371	<9.502
18d	<0.102	0.140	0.530	1.610	9.541	56b	0.130	0.250	0.750	1.660	10.204
21a	0.190	0.170	1.040	3.200	10.384	56c	<0.069	<0.084	<0.500	<0.354	<9.885
21b	<0.063	<0.111	0.240	1.350	9.903	56d	<0.072	<0.087	<0.105	<0.339	<9.480
21c	<0.090	<0.096	<0.099	<0.306	<9.333	56e	<0.078	<0.084	<0.111	<0.342	<9.447
21d	<0.090	<0.111	<0.147	<0.492	<9.684	59a	0.160	0.630	3.700	3.990	10.207
21e	<0.090	<0.111	0.180	0.440	9.701	59b	<0.066	<0.228	<0.135	<0.360	<8.882
22a	0.060	<0.093	0.100	<0.363	<8.505	59c	<0.102	<0.156	<0.114	<0.273	<8.879
22b	<0.075	<0.063	<0.174	<0.282	<8.549	59d	0.120	<0.650	<3.670	<3.840	<10.147
22c	<0.069	<0.081	0.250	0.810	8.882	59e	<0.069	<0.198	<0.096	<0.495	<10.482
22d	<0.057	<0.099	<0.156	<0.384	<9.689	61a	<0.072	<0.126	<0.150	<0.333	<8.861
22e	<0.075	<0.084	<0.159	<0.432	<9.739	61b	<0.078	<0.135	<0.129	<0.411	<7.822
30a	<0.144	<0.087	<0.090	0.550	<9.086	61c	0.290	0.500	5.640	12.010	10.467
30b	<0.084	<0.090	0.100	<0.438	<9.022	61d	<0.054	<0.090	<0.111	<0.243	<8.772
30c	<0.105	0.140	0.170	0.750	9.232	62a	<0.090	<0.180	<0.120	<1.910	<9.265
30d	<0.069	<0.069	<0.096	<0.297	<8.923	62b	<0.117	<0.180	0.200	1.720	9.322
31ac	0.130	0.750	4.980	6.690	10.365	62c	<0.105	<0.162	0.110	<1.320	<9.333
31b	0.078	0.060	0.081	0.384	8.862	62d	<0.108	<0.189	<0.090	<0.609	<9.004
31d	<0.072	<0.051	<0.087	<0.387	<10.510	67a	<0.123	<0.261	<0.190	<0.740	<9.811
31g	<0.090	<0.075	0.500	0.400	9.283	67b	0.170	0.280	1.010	2.590	10.333
33a	0.078	<0.102	<0.114	<1.900	<9.938	67c	0.080	<0.258	<0.210	0.900	<9.752
33b	<0.078	<0.126	<0.165	<2.073	<10.039	67d	<0.102	<0.252	<0.114	<0.387	<9.383
33c	0.130	0.240	0.680	1.840	10.193	68a	0.150	<0.114	0.420	1.700	9.019
33d	<0.096	<0.132	0.500	<2.400	<10.199	68b	<0.123	<0.090	<0.123	<0.312	<8.488

TABLE 2—*Continued*

HCG	I ₁₂ (Jy)	I ₂₅ (Jy)	I ₆₀ (Jy)	I ₁₀₀ (Jy)	L _{FIR} (L _⊙)	HCG	I ₁₂ (Jy)	I ₂₅ (Jy)	I ₆₀ (Jy)	I ₁₀₀ (Jy)	L _{FIR} (L _⊙)
37a	0.220	<0.093	0.560	2.300	10.082	68c	0.150	0.370	2.340	8.450	9.736
37b	0.200	0.290	0.660	2.130	10.091	68d	<0.087	<0.117	<0.156	<0.258	<8.430
37c	<0.096	<0.111	<0.093	<0.261	<9.284	68e	<0.105	<0.060	<0.180	<0.294	<8.488
37d	<0.090	<0.105	<0.081	<0.123	<8.957	69a	<0.096	<0.117	<0.153	<0.267	<9.567
37e	<0.086	<0.135	<0.108	<0.165	<9.104	69b	<0.102	0.440	2.260	4.240	10.734
69c	<0.102	<0.144	<0.141	<0.300	<9.537	92b	<0.230	0.220	0.850	2.780	10.069
69d	<0.099	<0.090	<0.144	<0.339	<9.626	92c	0.160	0.230	0.850	2.600	10.191
79a	<0.072	0.130	1.280	2.820	9.901	92d	0.150	<0.130	<0.850	<0.750	<9.962
79b	<0.072	<0.066	<0.130	<0.453	<9.041	92e	<0.090	<0.162	<0.087	<0.918	<9.547
79c	<0.078	<0.069	<0.105	<0.402	<8.912	96ac	0.660	1.930	5.650	8.440	11.093
79d	<0.063	<0.069	<0.093	<0.399	<8.961	96b	<0.138	0.150	<0.120	<0.573	<9.668
79e	<0.078	<0.110	<1.080	<2.370	<11.165	96d	<0.138	<0.144	<0.141	<0.534	<9.711
86a	<0.090	<0.162	<0.111	<0.378	<9.237	97a	<0.117	<0.195	<0.129	<0.384	<9.416
86b	<0.087	<0.114	<0.147	<0.552	<9.351	97b	<0.105	<0.123	0.150	0.860	9.629
86c	<0.069	0.230	0.380	1.670	9.724	97c	<0.165	<0.168	<0.123	<0.360	<9.236
86d	<0.081	<0.123	<0.174	<0.552	<9.409	97d	<0.129	<0.195	<0.200	<0.360	<9.383
87a	<0.120	<0.135	0.200	0.480	9.750	97e	<0.117	<0.165	<0.123	<0.426	<9.358
87b	<0.105	<0.165	<0.170	<0.400	<9.681	98a	<0.138	<0.180	<0.123	0.420	<9.509
87c	<0.111	<0.156	<0.102	<0.480	<9.624	98b	<0.138	<0.138	<0.108	<0.400	<9.484
87d	<0.118	<0.153	<0.220	<0.460	<9.882	98c	<0.120	<0.144	<0.114	<0.350	<9.482
88a	0.130	0.100	0.470	2.440	9.973	98d	<0.129	<0.144	<0.129	<0.460	<10.104
88b	<0.091	<0.075	0.140	<0.500	<9.343	99a	<0.108	0.100	<0.150	0.430	<9.643
88c	0.080	<0.120	0.360	2.030	9.889	99b	<0.110	<0.080	<0.183	<0.220	<9.585
88d	<0.069	<0.144	0.180	0.770	9.502	99c	0.100	<0.105	0.110	0.320	9.462
90a	0.440	0.960	5.850	12.420	10.108	99d	<0.102	<0.081	<0.123	<0.387	<9.573
90bd	0.210	0.310	3.430	8.530	9.917	99e	<0.114	<0.108	0.091	0.444	<9.681
90c	<0.054	<0.111	<0.144	<0.453	<8.567	100a	0.120	0.210	2.130	4.020	10.276
91ad	0.200	0.460	2.220	6.140	10.621	100b	<0.069	<0.117	<0.091	<0.444	<9.122
91b	0.120	0.240	2.060	3.830	10.526	100c	<0.072	<0.102	0.300	0.450	9.412
91c	<0.108	<0.138	<0.800	<1.000	<10.066	100d	<0.087	<0.087	<0.123	<0.774	<9.342
92a	<0.105	<0.210	0.450	<0.750	<7.918						

^aThe emission in HCG 54 is unresolved. The values correspond to the four galaxies of the group.

TABLE 3
PARAMETERS OF COMPARISON SAMPLES^a

Sample	N	Log L_B (L_\odot)	$\langle \mu_B \rangle$ (L_\odot/kpc^2)	log M_{H_2} (M_\odot)	log L_{FIR} (L_\odot)
Isolated	68	10.0	7.5	8.9	9.3
WP	43	10.5	7.7	9.6	10.3
SP	38	10.7	7.6	10.0	11.0
VC	58	9.9	7.6	8.8	9.3
CIG	212	10.2	7.6	...	9.5

^a L_B has been obtained as explained in § 2.2, and M_{H_2} and L_{FIR} as explained in § 3.1 and 3.2 respectively.

TABLE 4
RESIDUALS OF M_{H_2} RELATIVE TO THE M_{H_2} - L_B LAW^a

Sample	Median	Q ^b
ISO	0.04	0.17
WP	0.20	0.21
SP	0.10	0.27
VC	0.20	0.14
HCG-spiral	-0.32	0.65

^aSee Eq. 1 and § 3.1.

^bSemi-interquartile distance.

For a normal distribution $\sigma = 3/2$ Q.

TABLE 5
RESIDUALS OF L_{FIR} RELATIVE TO THE L_{FIR} - L_B LAW^a

Sample	Median	Q
CIG	-0.17	0.20
HCG, S	-0.22	0.50
HCG, S (det)	0.22	0.43

^aSee Eq. 2 and § 4.1.

TABLE 6
PARAMETERS OF $\text{LOG}(I_{25}/I_{100})$

Sample	Median	Q
CIG	-1.38	0.12
HCG, S	-1.12	0.17
SB+HII	-1.00	0.18

TABLE A-1
SCANPI SUMMARY OF RADIO^aQSOS

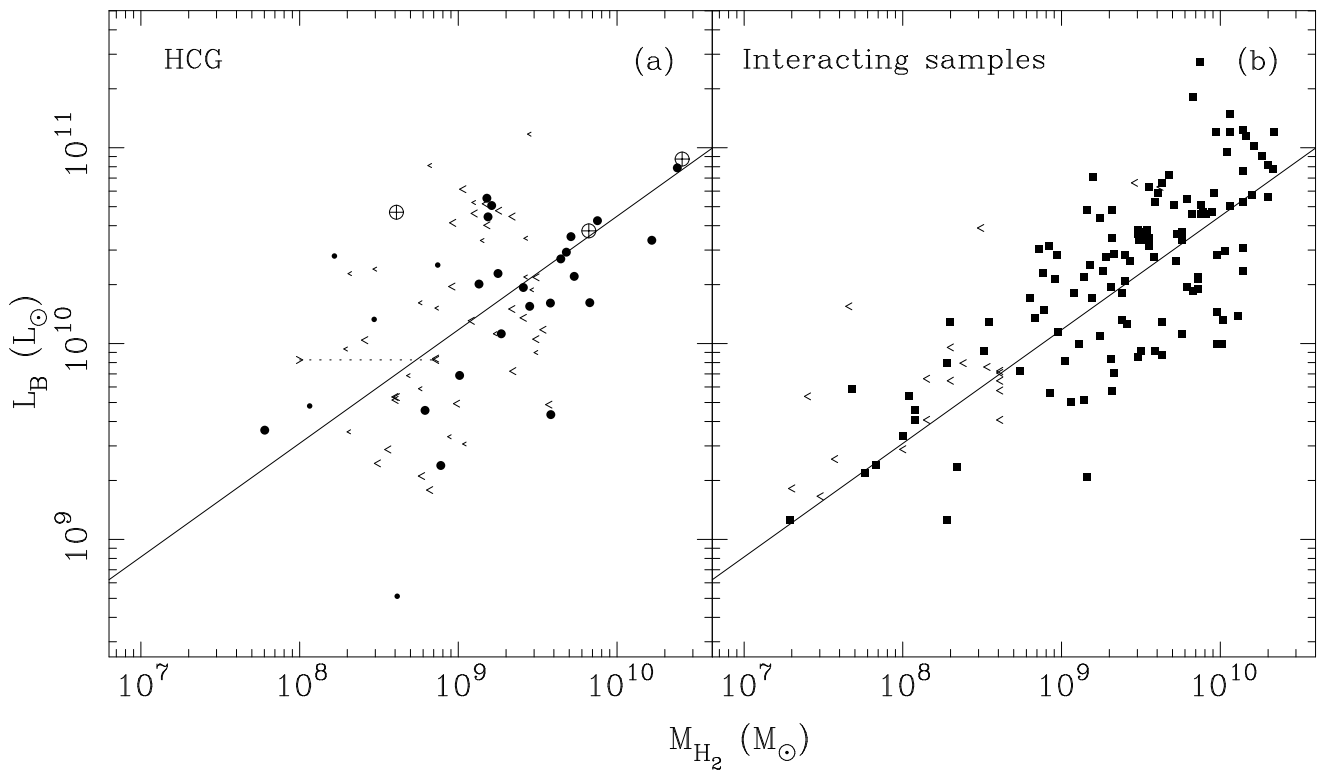
Source	$I_{60\mu}$ (N86) ^b (mJy)	$I_{60\mu}$ (SCANPI) (mJy)	S/N	miss (")	note
0007+106	213 ± 8	320 ± 56	5.7	-0.6	
0109+224		180 ± 39	4.4	-9.0	
0134+329	770 ± 9	830 ± 34	24.1	+0.0	
0234+285	187 ± 18	190 ± 56	5.7	-14.4	
0420-014	271 ± 16	450 ± 50	3.9	-2.4	
0438-436	120 ± 14	150 ± 33	4.6	+27.6	4 bright objects within 1'.5
0454-234		160 ± 30	5.2	-8.4	
0537-441	631 ± 25	460 ± 27	16.8	-2.4	
0736+017	133 ± 8	0 ± 52	0.0		
0738+313	145 ± 8	210 ± 34	6.1	+1.8	
0742+318	112 ± 8	100 ± 42	2.2	-27.6	3-4 similarly bright objects within 30"
0748+126	205 ± 17	250 ± 25	9.7	-28.8	several brighter objects within 1'
1219+285		250 ± 48	5.1	-8.4	a faint companion galaxy
1226+023	1805 ± 14	2060 ± 43	47.4	-1.8	
1253-055		220 ± 40	5.4	+6.0	
1404+286	652 ± 21	740 ± 35	20.6	-1.8	
1448+634	260 ± 40	270 ± 45	6.0	-1.2	
1514-241		360 ± 35	10.0	-11.4	spatially extended ($> 1'$)
1641+399	766 ± 18	720 ± 30	23.8	-1.2	
1652+398		90 ± 20	4.5	-3.6	
1656+053		220 ± 26	8.2	-2.4	
1739+522		100 ± 22	4.5	+6.6	
2059+034	174 ± 12	120 ± 40	3.0	+9.6	several faint sources within 1'
2201+315	126 ± 9	160 ± 46	3.4	+12.0	
2223-052	951 ± 16	680 ± 45	14.8	+1.8	
2251+158	179 ± 19	200 ± 59	3.4	+9.0	a bright companion
2254+074	155 ± 20	230 ± 38	6.1	-2.4	
2314+038	672 ± 52	720 ± 39	16.3	+8.4	a bright galaxy at 45" N
2334+282		190 ± 26	7.2	-0.6	

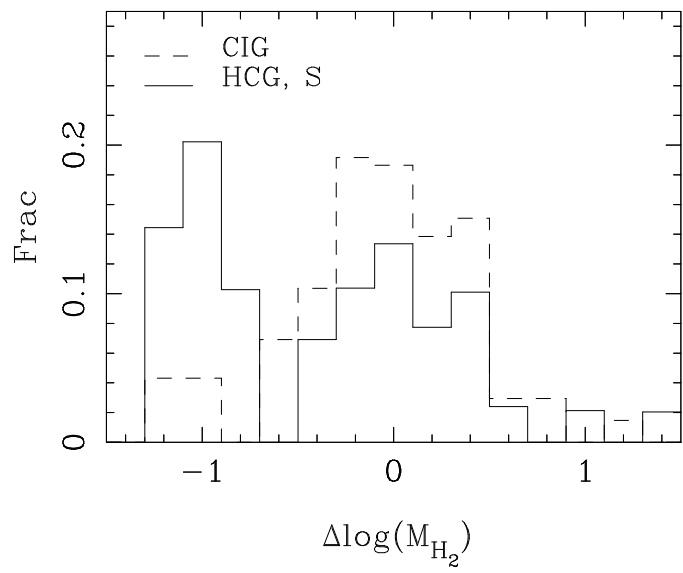
^aThe coordinates for the radio QSOS are taken from the VLA Calibrator Catalog and should be better than $0''.1$ in accuracy.

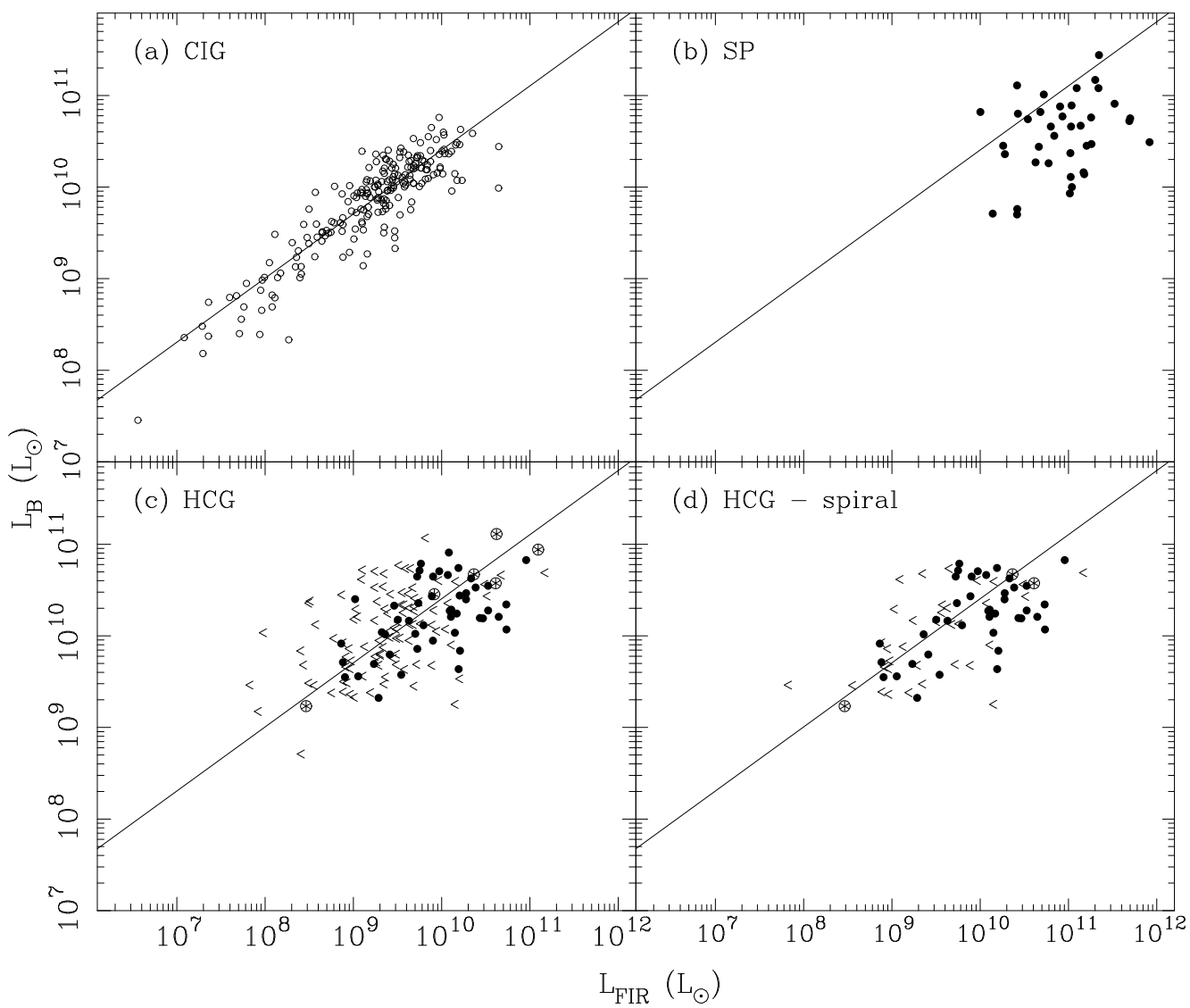
^bIRAS 60 μ m flux from the pointed observations by Neugebauer et al. (1986).

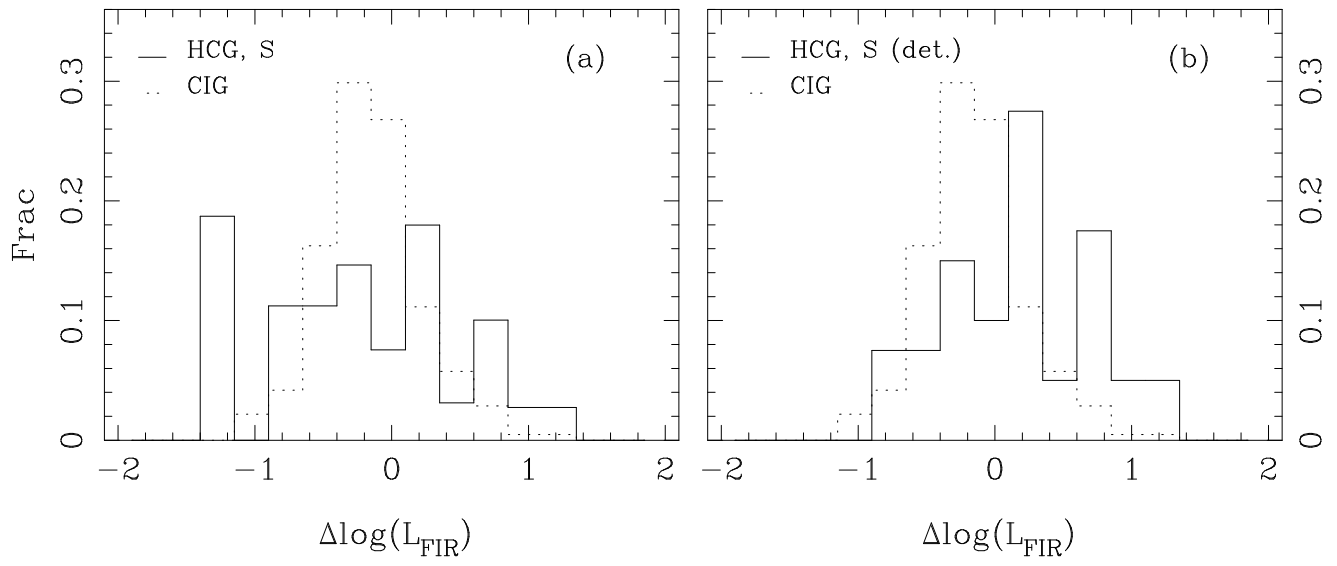
TABLE A-2
SCANPI DETECTION STATISTICS

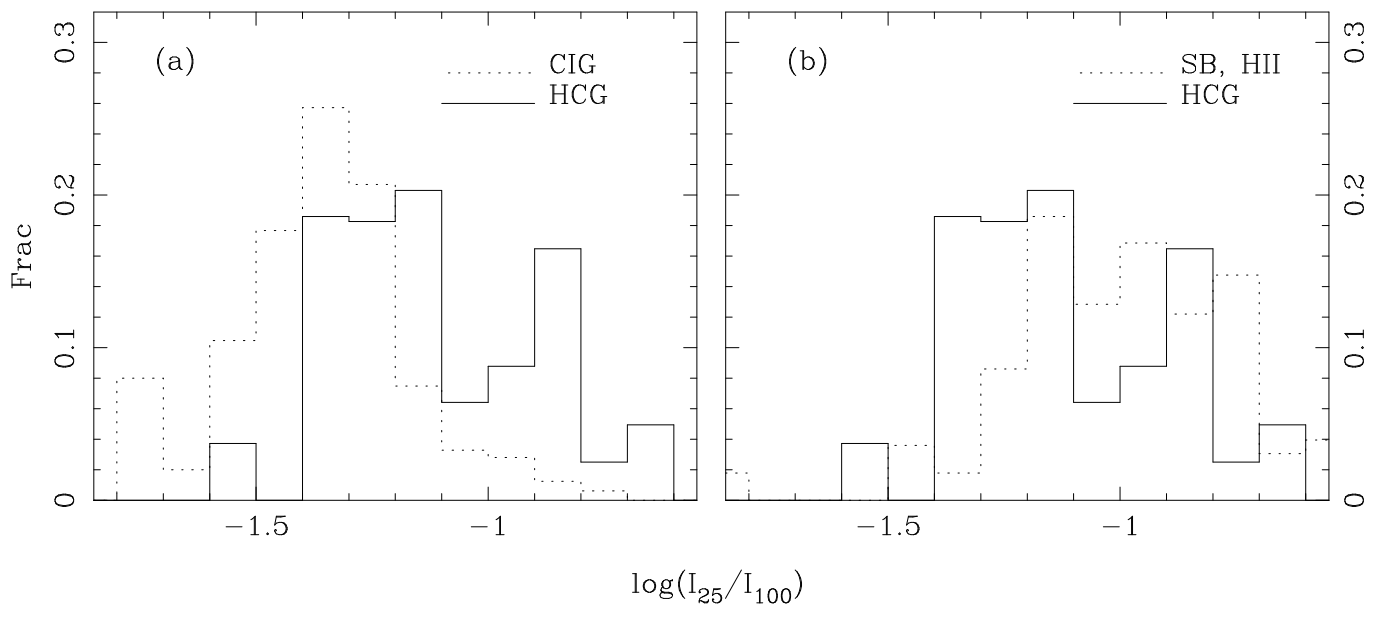
Source	S/N				
	<5	5-10	10-15	15-20	>20
QSO sample	8	11	2	2	4
HCG sample	13	12	5	5	37

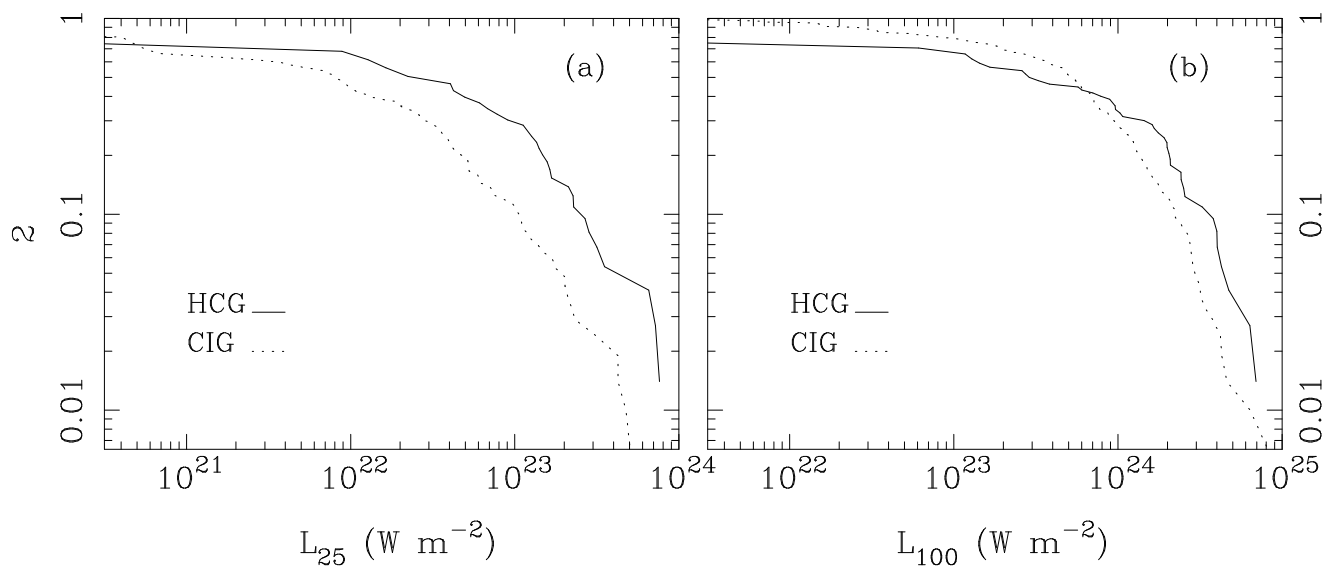


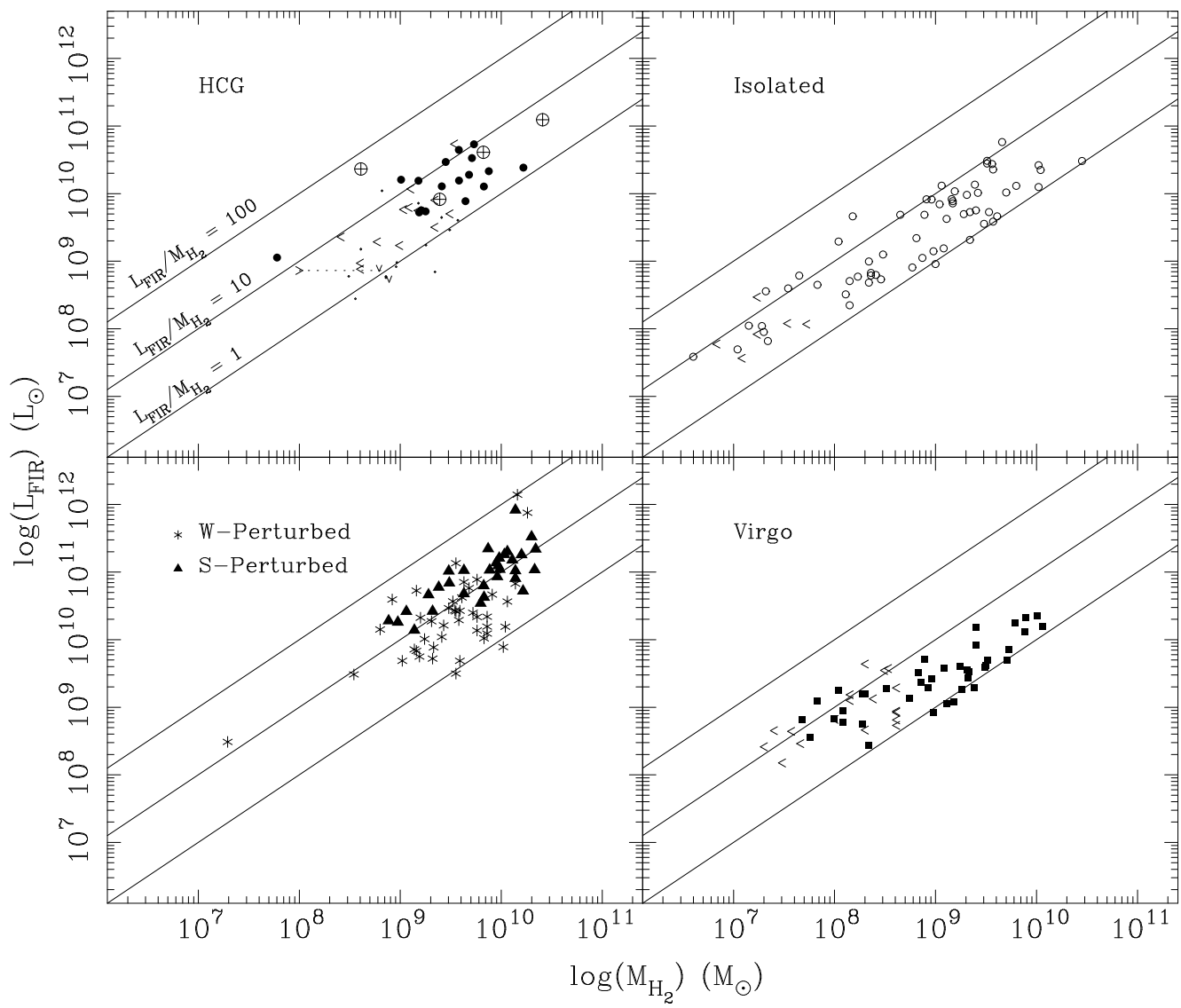












Effects of Interaction Induced Activities in Hickson Compact Groups: CO and FIR Study

L. Verdes-Montenegro

Instituto de Astrofísica de Andalucía, CSIC, Apdo. 3004, 18080 Granada, Spain.

(*lourdes@iaa.es*)

M. S. Yun

National Radio Astronomy Observatory¹, P.O. Box 0, Socorro, NM 87801 USA

(*myun@nrao.edu*)

J. Perea, A. del Olmo

Instituto de Astrofísica de Andalucía, CSIC, Apdo. 3004, 18080 Granada, Spain.

(*jaime@iaa.es, chony@iaa.es*)

and

P. T. P. Ho

Harvard-Smithsonian Center for Astrophysics, Cambridge, MA 02138 USA

(*pho@cfa.harvard.edu*)

Received 15 Jul 1997; accepted 6 Nov 1997

To appear in ApJ

¹The National Radio Astronomy Observatory is a facility of the National Science Foundation operated under cooperative agreement by Associated Universities, Inc.

ABSTRACT

A study of 2.6 mm CO $J = 1 \rightarrow 0$ and far-infrared (FIR) emission in a distance limited ($z < 0.03$) complete sample of Hickson Compact Group (HCG) galaxies was conducted in order to examine the effects of their unique environment on the interstellar medium of component galaxies and to search for a possible enhancement of star formation and nuclear activity. Ubiquitous tidal interactions in these dense groups would predict enhanced activities among the HCG galaxies compared to isolated galaxies. Instead their CO and FIR properties (thus “star formation efficiency”) are surprisingly similar to isolated spirals.

The CO data for 80 HCG galaxies presented here (including 10 obtained from the literature) indicate that the spirals globally show the same H_2 content as the isolated comparison sample, although 20% are *deficient* in CO emission. Because of their large optical luminosity, low metallicity is not likely the main cause for the low CO luminosity. The CO deficiency appears linked with the group evolution, and gas exhaustion through past star formation and removal of external gas reserve by tidal stripping of the outer HI disk offer a possible explanation.

The IRAS data for the entire redshift-limited complete sample of 161 HCG galaxies were re-analyzed using ADDSCAN/SCANPI, improving the sensitivity by a factor of 3-5 over the existing Point Source Catalog (PSC) and better resolving the contribution from individual galaxies. The new analysis of the IRAS data confirms the previous suggestion that FIR emission in HCG galaxies is similar to isolated, Virgo cluster, and weakly interacting galaxies. Their H_2 and FIR characteristics yield a star formation efficiency similar to that for these comparison samples. A factor two enhancement in the 25 μm to 100 μm flux

ratio among the HCG spirals is found, which suggests intense, localized nuclear starburst activity similar to HII galaxies.

A number of early-type galaxies in Hickson Compact Groups are detected in CO and FIR, lending further support to the idea that tidal interactions and tidally induced evolution of the groups and member galaxies are important in our sample.

Subject headings: galaxies: interactions — galaxies: groups — stars: formation — infrared: sources — interstellar medium: molecules

1. Introduction

Hickson (1982) identified 100 compact groups of galaxies by examining Palomar Observatory Sky Survey red plates. A recent complete spectroscopic survey has confirmed that 92 groups have at least three accordant members and 69 groups have at least four true members (Hickson et al. 1992). These compact groups constitute a unique environment to study galaxy interactions because of their high density and low velocity dispersion (300 to $10^8 h^{-2} \text{ Mpc}^{-2}$ and $\langle \sigma \rangle \sim 200 \text{ km s}^{-1}$, Hickson et al. 1992) that imply short dynamical lifetime ($\lesssim 10^9$ yrs). Members of these groups should experience almost continuous gravitational perturbations and not just encounters as in the case for pairs (Verdes-Montenegro et al. 1997). Violently interacting galaxies and close pairs show bluer optical colors (Larson & Tinsley 1978), strong FIR enhancements (Xu & Sulentic 1991; Surace et al. 1993) and higher radio continuum power (Hummel 1981; Hummel et al. 1990) relative to isolated galaxies, and similar enhancement in star formation and common occurrence of galaxy mergers are expected among HCG galaxies. However, a rather complex picture emerges from the observations. Zepf, Whitmore, & Levison (1991) and Moles et al. (1994) find from UBV photometry that the number of blue ellipticals produced by merger of spiral galaxies appears to be extremely low. Moles et al. (1994) and Sulentic & Rabaça (1994) concluded, based on optical data, that although star formation is enhanced with respect to isolated galaxies, it is of the same order as in pairs, and lower than in violently interacting pairs. Studies of cold gas at the 21 cm line indicate that HI is deficient and frequently disrupted or stripped from individual galaxies or form a single cloud surrounding the entire group (Williams & Van Gorkom 1995, and references therein; Huchtmeier 1997).

Molecular gas is generally thought to be the main ingredient in forming stars and thus of critical importance in understanding star forming activity in galaxies. Enhanced molecular gas content (as measured by M_{H_2}/L_B ratio) has been suggested by previous CO

surveys among tidally interacting systems, but we previously found that the larger M_{H_2}/L_B ratio reported for the bright interacting galaxies in the literature is entirely due to the non-linear dependence of M_{H_2}/L_B on L_B , independent of their environment, and their H_2 content is at the same level as isolated galaxies (Perea et al. 1997). In this paper, we report the first major survey of CO $J = 1 \rightarrow 0$ emission among the compact group galaxies in order to address the impact of their unique environment on their molecular ISM. The analysis of the CO data suggests that the majority (80%) of the Hickson compact group spiral galaxies show a normal level of CO emission, in agreement with a study based on 15 HCG galaxies by Boselli et al. (1996). Among the remaining 20% of the HCG spiral galaxies, a *deficiency* of CO emission is seen, and the CO deficiency appears to be associated with the entire individual groups rather than with odd individual members. The CO emission in two such CO deficient groups, HCG 31 and HCG 92 (Stephans’ Quintet), are mapped at high angular resolutions using the Owens Valley Millimeter array and found to be highly disturbed (Yun et al. 1997).

We also present a new analysis of the IRAS data for our entire distance limited sample in order to complement the CO study. In an earlier study, Hickson et al. (1989b, hereafter HMPP) suggested enhancement of far-infrared emission among the HCG galaxies based on the analysis of IRAS Point Source Catalog (PSC). However, Sulentic & de Mello Rabaça (1993) and Venugopal (1995) have argued that the same data suggest a normal level of FIR emission if the source confusion is taken into account. The new analysis uses ADDSCAN/SCANPI data, which is 3-5 times more sensitive than IRAS PSC and allows a better resolution of source confusions. IRAS HIRES maps are also used to resolve the confusion problem in some cases. Our new analysis find the FIR luminosity distribution of HCG galaxies indistinguishable from isolated galaxies and demonstrates that an analysis based on IRAS detected subsample alone can lead to an erroneous conclusion of FIR enhancement. The suggestion of enhanced nuclear star formation activity based on radio

continuum observations by Menon (1995) is supported by the corresponding enhancement in the IRAS 25 μm flux.

The organization of the paper is as follows. Our distance limited complete sample of Hickson compact groups, the CO observations of a representative subset, the IRAS data analysis, and the details of the comparison samples are discussed in §2. It is followed by the results of the CO (§3) and FIR (§4) analysis, and star formation efficiency (§5). The interpretation of the CO and FIR analysis are discussed in §6 in the context of tidal perturbations and other effects in the compact group environment. The analysis of IRAS ADDSCAN/SCANPI data on radio-loud QSO’s is utilized to evaluate the formal uncertainties and statistics associated with this data product, and this is discussed separately in the Appendix.

2. OBSERVATIONS AND DATA ANALYSIS

2.1. Sample Selection and Characteristics

To conduct the analysis of CO and FIR emission in Hickson compact groups we have selected a statistically complete sample of 39 (out of 100) groups, including 172 galaxies, that satisfy the following criteria:

(1) $\mu_G \leq 24 \text{ mag arcsec}^{-2}$: a mean group brightness limit stated to be “complete” by Hickson (1982);

(2) $z \leq 0.03$: a distance limit to ensure large galaxy angular sizes and less source confusion; and

(3) $N \geq 3$: a minimum membership requirement as determined in Hickson et al. (1992).

The requirements (1) & (2) are complementary and limit the sample to only the nearest groups where the majority of the members are sufficiently separated for ADDSCAN/SCANPI analysis and CO observations. These criteria also reduce the redshift bias introduced in the original selection of the groups by Hickson (1982) such as the inclusion of poor clusters at high redshifts. Requirement (3) is used to ensure that the selected objects are real physical groups. Spiral and Irregular galaxies comprise 56% (89 out of 161) of all galaxies in our complete sample while the remaining 44% are E’s and S0’s.

The CO observations presented here include a subset of 80 galaxies (including 10 obtained from the literature, see Table 1) in 24 groups in our complete sample. The groups observed in CO are randomly chosen from our complete sample in the sense that the groups matched well with the telescope time allocation were observed. A special effort was made to observe every accordant redshift member in each group to avoid any luminosity bias. Nine galaxies in higher redshift groups HCG 35, HCG 85 and HCG 95 ($z \sim 0.03-0.05$) are also observed for a related study, and the results are reported here, but only the low redshift subsample is included in our statistical analysis. The analysis of the FIR properties is conducted for the entire complete sample for which the IRAS observation is available. HCG 42 and HCG 51 fall in the IRAS data “gap”, and we have obtained ADDSCAN/SCANPI data on the remaining 37 groups (161 galaxies) using the XSCANPI utility.

2.2. CO Observations

The CO emission is searched in a total of 70 galaxies in our distance limited sample, plus 9 galaxies in the three high redshift groups HCG 35, HCG 85 and HCG 95 ($z \sim 0.03-0.05$). The majority (74 out of 79) are observed with the NRAO 12-m telescope at Kitt Peak during three separate observing sessions between October 1995 and October 1996,

and two galaxies are observed using the 37-m radio telescope at Haystack Observatory² in January 1996. Both telescopes were equipped with SIS receivers, with typical system temperatures of 300-500 K (SSB) and 600-900 K (SSB), respectively. The beam sizes at 115 GHz are 55'' and 18'' (FWHM). The 500 MHz filter banks at 2 MHz resolution and 600 MHz hybrid digital spectrometer with 0.78 MHz resolution were used to record the NRAO 12-m telescope data, and a 320 MHz auto-correlation spectrometer at 1.25 MHz resolution was used for the Haystack observations. In addition, ¹²CO (J = 2→1) observations of 3 galaxies in HCG 61 were obtained at the Caltech Submillimeter Observatory³ 10.4-m telescope at Mauna Kea, Hawaii, in April 1996. The facility SIS receiver with typical system temperature of 400 K (SSB) was used with 1024 channel 1.5 GHz acousto-optical spectrometer, and the beam size at 230 GHz was about 30''.

The observed positions correspond to either the radio continuum source locations reported by Menon (1985, 1995) when available or the optical positions given by Hickson (1993). Pointing was checked frequently by observing nearby planets or quasars, and the rms pointing uncertainty of the telescopes was better than 3''-5'' in all cases. All observations were made using beam switching mode with a typical beam throw of 3' at ~1 Hz frequency, and resulting flat and well-behaved spectra required only linear baseline removal in most cases. For the analysis, two polarization spectra are averaged and Hanning smoothed to 15-20 km s⁻¹ velocity resolution in order to improve signal to noise ratio. The CO spectra of the detected galaxies are shown in Fig. 1, including those of IC 883, NGC 2738, and NGC 6090 taken for system tests. The CO spectrum in NGC 2738 has never been

²Radio Astronomy at Haystack Observatory of the Northeast Radio Observatory Corporation is supported by the National Science Foundation

³The Caltech Submillimeter Observatory is funded by the National Science Foundation under contract AST-9313929.

reported previously, but its bright CO line is not surprising given its bright 60 μm flux.

Out of 80 galaxies observed, CO emission is detected in 28 resolved galaxies and 3 unresolved pairs. Good upper limits are obtained for the remaining 48 galaxies and the high redshift group galaxies. The detection rate is 50% for spiral galaxies and 20% for early-type galaxies. The observed and derived quantities such as CO central velocity (column 6), brightness temperatures in main beam scale (column 7), line width (column 8) and CO integrated intensity (column 9) are listed in Table 1. The optical size of the galaxies are larger than the observed beam in 15 cases, and $\sim 10\%$ correction to the total fluxes are made assuming an exponential distribution for gas (see Young et al. 1995). Because most published CO surveys are biased toward IR or optically luminous isolated spirals, CO data is reported on only 14 HCG galaxies in the literature. Four galaxies (H7c, H90a, H90b, & H90d) are observed again to confirm our NRAO 12-m observations, and the correction technique for small observing beam has produced consistent results with the published measurements.

2.3. ADDSCAN/SCANPI Analysis of the IRAS Data

By definition, Hickson compact groups consist of several galaxies located within a few arcmin diameter region, and differentiating contribution from individual galaxies is difficult in the IRAS full resolution data (angular resolution $\sim 4'$ at 100 μm). In an earlier study HMPP suggested enhancement of far-infrared emission among HCG galaxies based on the analysis of IRAS PSC data. However, Sulentic & de Mello Rabaça (1993) and Venugopal (1995) argued that the same data suggest a normal level of FIR emission if the presence of two or more IR sources in several unresolved HCGs are taken into account. Two extra steps are taken here to improve the analysis of the IR properties of Hickson compact group galaxies: 1) by obtaining higher spatial resolution information with improved sensitivity

using IRAS ADDSCAN/SCANPI data; and 2) by limiting our statistical analysis to a complete sample of nearby ($z \leq 0.03$) groups only and minimizing the luminosity bias.

ADDSCAN/SCANPI is a one-dimensional co-adder of the calibrated IRAS survey data available at Infrared Processing and Analysis Center. It performs co-addition of all scans that passed over a specific position in the IRAS raw survey data and produce a scan spectrum along the average scan direction with flux scaling accurate to a few percent of PSC. While the intrinsic resolution of ADDSCAN/SCANPI is about $1'$ at 60μ band, the centroid of the source can be determined with much higher accuracy ($1\sigma \sim 7''$ for $S/N > 5$ – see Appendix and Surace et al. 1993). Furthermore, ADDSCAN/SCANPI data is about 3-5 times more sensitive than IRAS PSC, and we could achieve detections of fainter IRAS sources as well as placing better upper limits on undetected sources. The results of ADDSCAN/SCANPI analysis of $12\mu\text{m}$, $25\mu\text{m}$, $60\mu\text{m}$ and $100\mu\text{m}$ bands for 161 galaxies in 37 Hickson compact groups are given in Table 2. For several compact groups with a high degree of confusion (e.g., HCG 33, HCG 40, HCG 56, HCG 88), $60\mu\text{m}$ HIRES maps are obtained to identify the IR sources.

Among the distance limited complete sample of 39 HCGs, all but one group (HCG 46) have at least one galaxy detected in our XSCANPI analysis while no IRAS data is available in two groups (HCG 42 & 51). At least 67 and 61 out of 161 galaxies are detected at 60 and 100 μm band, respectively, including five unresolved pairs (HCG 31ac, HCG 38bc, HCG 90bd, HCG 91ad, HCG 96ac) and one unresolved quartet (HCG 54). The comparison of our results with the HIRAS analysis of HCG galaxies by Allam et al. (1996) clearly demonstrates that ADDSCAN/SCANPI process is more sensitive for detection than HIRAS process – this is expected since HIRAS and other methods using maximum likelihood estimator require a high S/N. For example, among the same 36 groups where we report at least one IRAS detection, Allam et al. report non-detection in eight groups (HCGs 22,

30, 62, 86, 87, 97, 98, 99). Among 91 commonly resolved galaxies, the total number of detections reported in our/their data at $12\mu\text{m}$, $25\mu\text{m}$, $60\mu\text{m}$ and $100\mu\text{m}$ are 30/11, 29/15, 44/37 and 39/33, respectively. On the other hand, the accuracy of the flux determination is mutually verified since the difference between the measured fluxes for the commonly detected galaxies has a zero median and nearly always within 2σ of the median.

2.4. Comparison Samples

In order to investigate whether the observed CO and FIR characteristics of HCG galaxies show any observable effects of being subjected to continuous tidal disruptions in a compact group environment, comparison samples of isolated and interacting galaxies are constructed, matching absolute magnitude distribution whenever possible. For the CO study we have compiled from the literature an extensive comparison sample of 207 galaxies of varying interaction classes and environment representing a wide range of luminosity ($10^{8.6} L_{\odot} < L_B < 10^{11.4} L_{\odot}$), and for which FIR, CO and B luminosity are available. Because many nearby galaxies typically subtend several arcmin in size and are much larger than the beams of the observed telescopes, the comparison data consist mostly of CO surveys using at least partial mapping (e.g. Young et al. 1995). The “isolated” galaxy sample consists of 68 objects compiled from the distance limited survey of Nearby Galaxies Catalog (Tully 1988) by Sage (1993) and interaction class 0 objects of Solomon & Sage survey (1988; hereafter SS88). Morphological types range from Sa to Sd with $10^{8.6} \geq L_B \geq 10^{10.9} L_{\odot}$. This sample lacks completeness because CO surveys found in the literature are frequently biased towards infrared luminous galaxies, but a wide range of luminosity represented allows us to characterize the CO emission in the isolated environment. Only upper limits are available for six galaxies. The “weakly perturbed” (WP) galaxy sample consists of 43 galaxies including interaction class 1, 2 & 3 objects in SS88 and interaction class 2

objects of IRAS Bright Galaxy Sample by Sanders, Scoville, & Soifer (1991). The “strongly perturbed” (SP) galaxy sample consists of 38 galaxies including interaction class 4 objects in SS88, IRAS Bright Galaxy Sample interaction class 3 & 4 objects, and closely interacting pairs from Combes et al. (1994). The definitions of “weakly perturbed” and “strongly perturbed” are given in the references listed above – SP galaxies are generally distinguished from WP galaxies as the final stages of mergers. In addition, we have constructed a Virgo cluster (VC) sample made of 58 bright (Kenney & Young 1988a, 1988b) and faint spirals (Boselli, Casoli, & Lequeux 1995). For 3 galaxies in SP and 18 galaxies in VC sample, only CO upper limits are available. All the data have been normalized to a common CO-to-H₂ conversion factor (see § 3) and $H_0 = 75 \text{ Mpc}^{-1} \text{ km s}^{-1}$.

Owing to an extensive database available in IRAS, the construction of a matching comparison sample for the FIR study is much easier. The FIR comparison sample consists of 212 “class 0” (no companion) galaxies from the Catalog⁴ of Isolated Galaxies (CIG) by Karachentseva, Levedeb, & Shcherbanovskij (1973) with redshift and blue luminosity distributions matching that of the HCG sample. The optical luminosity has been derived from the B_T⁰ magnitude from the RC3 catalogue (de Vaucouleurs et al. 1991), correcting for galactic absorption (using the extinction value given by Burstein & Heiles 1984 with the reddening law from Savage & Mathis 1979) and internal extinction and K-correction (de Vaucouleurs et al. 1991) using the redshift given in NED⁵. The B_T⁰ data for HCG galaxies are found in Hickson, Kindl & Auman (1989b, hereafter HKA), but they are corrected

⁴The Catalogue has been obtained at CDS (Centre de Données Astronomiques de Strassbourg)

⁵The NASA/IPAC extragalactic database (NED) is operated by the Jet Propulsion Laboratory, California Institute of Technology, under contract with the National Aeronautics and Space Administration

by 0.1 mag to account for the systematic offset between HKA and RC3 (Moles et al. 1994, Fasano & Bettoni 1994). Data for the other samples are obtained through the NED database.

The summary of physical properties for all CO and FIR comparison samples are given in Table 3, and the cumulative optical luminosity functions are shown in Figure 2. Given its completeness and depth, CIG sample is well suited for characterizing the optical luminosity distributions of the other samples. The optical luminosity distribution of HCG spirals closely coincides with those of CIG sample (98% probability in a logrank test), and the CO observed subsample has slightly larger optical luminosity (Fig. 2a). Interacting galaxies (WP, SP) show slightly larger optical luminosity due to their biased selection as bright infrared sources (Table 3). Both isolated CO comparison sample and Virgo cluster sample lack galaxies at high luminosity end. Because 2/3 of the isolated CO comparison sample come from the distance limited survey by Sage (1993), this lack of bright spirals is easily explained by the small volume sampled and the local galaxy luminosity function.

While all comparison samples are composed of spiral galaxies only, 39% of our HCG sample (24% for the CO subsample) are E/S0 types. Thus we analyze spiral and early-type galaxies separately below.

3. CO Emission and Molecular Gas Content among HCG Galaxies

Molecular hydrogen mass, M_{H_2} , is derived using a standard CO-to- H_2 conversion, $N_{H_2}/I_{CO} = 3 \times 10^{20} \text{ cm}^{-2} (\text{K km s}^{-1})^{-1}$ and is given by $M_{H_2} = 4.82 I_{CO} d_B^2 M_\odot$, where I_{CO} is velocity integrated CO flux in K km s^{-1} and d_B is the half-power beam diameter in parsec (Sanders et al. 1991). The derived molecular gas masses for the 27 detected and resolved HCG accordant galaxies are listed in Table 1, and they range between $4.6 \times 10^7 M_\odot$

(HCG 44d) and $2.4 \times 10^{10} M_{\odot}$ (HCG 96a, NGC 7674) with a median M_{H_2} mass of about $2 \times 10^9 M_{\odot}$. Three unresolved pairs HCG 31ac, HCG 38bc, and HCG 90bd do not have particularly high total gas masses for their optical luminosity.

3.1. Spiral HCG Galaxies

In order to examine for any enhancement or deficiency in CO emission among the HCG spirals, derived molecular gas mass (M_{H_2}) is plotted against blue luminosity (L_{B}) for HCG, VC, WP, and SP sample spirals in Figure 3 along with a solid line corresponding to the power law relation derived from the isolated and field spirals in our earlier study (Perea et al. 1997). Because these two quantities are strongly non-linearly related, the common practice of normalization by optical luminosity as a measure of molecular gas enhancement (e.g. Braine & Combes 1993) is an inadequate and misleading way to evaluate enhancement or deficiency of molecular gas content, and measuring the deviation from this power law relation should be a more meaningful test. Accordingly the median value of the residuals ($\Delta[\log(M_{\text{H}_2})]$) with respect to the isolated galaxies template are tabulated in Table 4 along with the semi-interquartile distance which measures the dispersion of the distribution (for a normal distribution, $\sigma = 3/2 \text{ Q}$). Upper limits have been taken into account using Astronomy SURVival Analysis (ASURV⁶). The deviation of the residuals from zero is statistically negligible for both weakly and strongly interacting pairs and cluster galaxies. Figure 3 suggests that HCG galaxies follow the same non-linear M_{H_2} - L_{B} relation, but the

⁶Astronomy Survival Analysis (ASURV) Rev 1.2 package is a generalized statistical analysis package which implements the methods presented by Feigelson & Nelson (1985) and Isobe et al. (1986) and are described in detail in Isobe & Feigelson (1990) and La Valley et al. (1992)

median value of $\Delta[\log(M_{\text{H}_2})]$ is slightly lower (1.3σ) compared with the CIG sample. The histogram of the residuals of the resolved HCG spiral galaxies (Fig. 4) demonstrates more clearly that there is a subsample of H_2 deficient galaxies compared with isolated galaxies. This subsample includes 10 galaxies in total (6 upper limits) and accounts for about 20% of all the surveyed HCG spirals.

The observed deficiency of molecular gas among the HCG spirals is *not* because they are low metallicity dwarfs – CO deficient spiral galaxies have $L_B > 10^{10} L_\odot$ and similar luminosity distribution as WP and SP sample. A telling clue to the physical reality and possible causes of the CO deficiency is that all three observed galaxies in HCG 92 (b, c, & d) are CO deficient – nearly ten times less CO emission than expected for their luminosity. Similarly, the unresolved pair H31ac, which is also one of the densest groups in Hickson catalog, displays a factor 30 deficiency in CO emission for its optical luminosity. We have studied both HCG 31 and HCG 92 with the OVRO interferometer (Yun et al. 1997) in order to better understand their faint CO emission and found that the CO emission is highly asymmetric and disturbed. Strong tidal disruptions likely play an important role in producing such morphology, but the actual physical mechanism for producing reduced CO emission is uncertain. Possible explanations for the CO deficiency in these most compact (thus presumably the most evolved) groups include the exhaustion of gas supply through tidally induced massive star formation, and they are discussed further in § 6.

3.2. E/S0 HCG Galaxies

Among the distance limited complete sample of HCG galaxies where CO emission is searched, there are 24 early-type galaxies with Hubble type E or S0, and 5 galaxies are detected with inferred molecular gas masses of $(1.2\text{--}24.8)\times 10^8 M_\odot$. Because only a limited number of ellipticals have been observed in CO previously, the statistical importance of

a 20% detection is not clear. However, such presence of cold gas in elliptical galaxies is generally attributed to a merger or accretion of a gas-rich companion (Wiklind, Combes, & Henkel 1995; Huchtmeier & Tammann 1992; Lees et al. 1991). The two CO detected elliptical galaxies HCG 90b and HCG 90c are very close to an irregular galaxy HCG 90d, which is in projected contact with HCG 90b and joined by a tail-like feature with HCG 90c (Longo et al. 1994). HCG 90b and HCG 90d are unresolved by our beam, and the spectrum (Fig. 1) is well centered at the velocity of the irregular galaxy. However, the CO observations of HCG 90b by Huchtmeier & Tammann (1992) with a smaller beam also support that a significant part of the molecular gas is associated with the elliptical galaxy since their beam does not include HCG 90d. This may also be the case in HCG 90c, as suggested by its optical bridge with HCG 90d. This observation is consistent with a general expectation that mergers or accretions can readily occur in compact group environment. Another CO detected source HCG 68a is a lenticular galaxy which is also an X-ray and FIR source. It is also in close contact with an elliptical companion HCG 68b, and the only spiral companion in the group is 4' away. HCG 61a was originally classified as a spiral by Hickson (1993), but it is classified as an elliptical by Rubin et al. (1991) and as a lenticular in RC3. The molecular gas in this galaxy probably originated from a late type companion such as HCG 61c (Sbc).

4. Infrared Properties of HCG Galaxies

4.1. Far Infrared Luminosity Distribution

The UV and optical photons emitted by massive young OB stars are absorbed and re-radiated in the far-infrared by dust. Therefore infrared emission provides a vital clue in the study of star formation activity and the surrounding medium. FIR luminosity is computed from the IRAS measurements as $\log(L_{FIR}/L_{\odot}) = \log(FIR) + 2\log(D) + 19.495$,

where D is distance in Mpc and $FIR = 1.26 \times 10^{-14}(2.58I_{60} + I_{100}) \text{ W m}^{-2}$ (Helou et al. 1988). The λ 12 μm , 25 μm , 60 μm , and 100 μm fluxes and derived FIR luminosity (L_{FIR}) are listed in Table 2. A total of 161 HCG galaxies are examined, and 5 pairs (HCG 31ac, HCG 38bc, HCG 90bd, HCG 91ad and HCG 96ac) and one quartet (HCG 54) are still unresolved by ADDSCAN/SCANPI. For these cases, the sums of FIR fluxes are listed in Table 2. The number of IRAS detected individual galaxies and unresolved pairs/quartet are respectively 35/5 at 12 μm ($\geq 25\%$), 36/6 at 25 μm ($\geq 26\%$), 61/6 at 60 μm ($\geq 42\%$) and 55/6 at 100 μm ($\geq 38\%$). Among the 75 galaxies undetected by IRAS, 67 galaxies (75%) are classified as E or S0 and are not expected to emit in far-infrared above the IRAS sensitivity. The remainder have $m_B > 14.7$, below the IRAS detection limit derived through the L_{FIR} - L_B relationship (see Figure 5).

In the conservative assumption that FIR emission in unresolved pairs comes from only one galaxy, 68% (25/37) of the groups contain more than 1 IRAS source, and 29% (10/37) contain at least 3 IRAS sources. This confirms the inference made by Sulentic et al. based on source statistics that more than one galaxy contributes to the FIR emission detected by IRAS. HCG 46 is the only Hickson compact group without any FIR source detected by SCANPI ($\sigma \sim 30 \text{ mJy}$ at 60 μm). For the statistical analysis of FIR properties, 149 galaxies in 37 Hickson groups are included after excluding 12 galaxies with a discordant redshift.

The FIR luminosity of HCG galaxies has been evaluated in a similar way as for the molecular content. There is a known close correlation between L_{FIR} and L_B (see Bothun, Lonsdale, & Rice 1989; Dultzin-Hacyan et al. 1990), and the blue luminosity of the CIG sample of isolated galaxies can be described as

$$\log L_B = (0.70 \pm 0.03) \log L_{FIR} + (3.4 \pm 0.2) \quad (1)$$

This agrees well with the relation found for the isolated galaxy sample of Perea et al. (1997), $L_B \propto L_{FIR}^{0.65 \pm 0.09}$. Again, the normalization using optical luminosity still leaves a residual

dependence of L_{FIR}/L_B on L_B so that brighter galaxies will have intrinsically larger values for this ratio independently of environmental effects. The presence of any FIR enhancement among HCG galaxies is examined by comparing their $L_B - L_{FIR}$ distribution with the CIG and SP comparison sample in Figure 5. The well known FIR enhancement among the SP sample is clearly shown in Fig. 5b. The data for all HCGs galaxies are shown in Figure 5c, and HCG spiral galaxies are shown separately in Figure 5d. These figures suggest that HCG spiral galaxies follow the same trend as the CIG galaxies. The distribution of residuals $\Delta[\log(L_{FIR})]$ relative to the power law in Eq. 1 is shown in Figure 6a for the CIG and HCG spirals samples, and the corresponding median and semi-interquartile distances are listed in Table 5. Both samples have the same median value, with a larger dispersion for the HCGs galaxies. We conclude that HCG spirals as a group do not show a significant enhancement in their FIR emission with respect to CIG galaxies. If only the detected galaxies are included in the analysis, an apparent enhancement by a factor 3 is suggested (see Tables 5, Fig. 6b). However, this is due to a well known luminosity and detection bias, and all upper limits for the low FIR luminosity galaxies have to be taken into account for a proper analysis.

In summary, no significant enhancement in FIR emission is found among the HCGs spirals. This contradicts the earlier findings by HMPP, and the reason for the contradiction is in part due to the presence of more than one FIR source in many of the groups as suggested by Sulentic & De Mello Rabaça (1993) and Venugopal (1995). At least 68% of the groups contain more than 1 IRAS source and 29% have at least 3 IRAS sources, and assigning FIR fluxes to a single galaxy have lead HMPP to over-estimate the FIR emission per galaxy.

Only 17 out of 71 early-type galaxies are detected by IRAS, and this is similar to the detection rate found for other early-type samples (Marston 1988). FIR emission from

early-type galaxies is usually attributed to dusty ellipticals and S0's, as a result of merger or accretion processes (Marston 1988). Six galaxies are detected at least in 3 IRAS bands, and they all show peculiarities. Four of these galaxies are the 1st ranked in the group or the brightest early-type member. HCG 37a is a radio and X-ray source with a rapid rotating disk in the center, and [N II] emission and ellipticity variations are reported (Rubin, Hunter, & Ford 1991; Bettoni & Fassano 1993). The S0 galaxy HCG 56b has a warped disk connecting with that of the S0 companion HCG 56c and is also a radio continuum source (Rubin et al. 1991; Menon & Hickson 1985). HCG 68a is a radio and X-ray source and has associated 21cm HI emission (Williams & Rood 1987), and CO emission is detected by our survey. HCG 79a is a radio continuum and 21cm HI source and is crossed by a strong dust lane, suggesting an accretion from a spiral companion HCG 79d. HCG 86c is classified as SB0 and is detected in 25 μm , but spectroscopic measurements of the Mg₂ band suggest a metallicity characteristic of a normal elliptical galaxy ($M_g = 0.29$, $\sigma_v = 173 \text{ km s}^{-1}$).

4.2. I_{25}/I_{100} Ratio – an Indicator of Enhanced Nuclear or Starburst Activity

The flux ratio between IRAS 25 μm and 100 μm bands, I_{25}/I_{100} , is an useful indicator of nuclear or starburst activity (Dultzin-Hacyan et al. 1988, 1990). The histograms of I_{25}/I_{100} ratio for the CIG sample and HCG spirals are shown in Figure 7, excluding the unresolved pairs. The data for a sample of HII, blue compact, clumpy irregulars and starburst galaxies from Dultzin-Hacyan et al. (1990) are also shown for comparison. Only the galaxies detected at least at 100 μm are considered since the ratio becomes too uncertain if undetected at 100 μm . Among the samples considered, 45% of CIG sample galaxies and 72% of HCG galaxies are detected at 25 μm band. Galaxies with only upper limits at 25 μm are also included in the analysis.

The distributions of I_{25}/I_{100} ratio for the CIG and HCG sample are different at 99.99%

level according to the logrank and Peto-Prentice generalized Wilcoxon tests included in ASURV which are known to be the most robust in measuring the degree of discrepancy between two cumulative distribution functions in the presence of lower or upper limits. The median value of the I_{25}/I_{100} ratio for HCGs galaxies is a factor 2 larger than for CIG sample (Table 6) and similar to the compact starburst sample from Dultzin-Hacyan et al. (1990). Including only the 100 μm detected galaxies in the analysis has little effect on this conclusion because the comparisons of the cumulative functions including all data show that the enhancement in the HCG sample is in the 25 μm emission while the 100 μm cumulative luminosity functions are identical (see Figure 8).

The enhanced I_{25}/I_{100} ratio among HCGs galaxies indicates enhanced and localized UV radiation field, due to either intense local star formation or by presence of an AGN. The number of known Seyfert galaxies among HCGs galaxies is small (9% in our complete sample), and therefore the bulk of the excess seems to be due to local starbursts, presumably in the nuclear region as suggested by the enhanced nuclear radio continuum emission (Menon 1995). A detailed spectrophotometric study is needed to confirm this result. This evidence for enhanced localized starburst is still compatible with the conclusion of normal level of FIR emission among HCG galaxies if the activity responsible for enhanced 25 μm emission is localized compared to the over-all distribution of gas and dust in each galaxies, as in HII and Markarian galaxies.

5. Star Formation Efficiency (L_{FIR}/M_{H_2})

A linear correlation between the observed FIR luminosity and the total CO luminosity is well documented by various previous surveys, and the L_{FIR}/M_{H_2} ratio is sometimes quoted as “star formation efficiency” (SFE; see Young & Scoville 1991 and references therein). The total FIR luminosity of the CO observed subsample is plotted as a function

of total derived H_2 mass along with those of the comparison galaxies in Figure 9, and the results are quantified through the statistical analysis described in Perea et al. (1997) in order to examine whether HCGs have a star formation efficiency similar to strongly interacting galaxies. The “correlation” between CO and FIR is a rather broad tendency spanning *two orders of magnitudes* in L_{FIR}/M_{H_2} ratio. On the other hand, individual interaction sub-classes, with the exception of SP sample, occupy a much narrower strip of area between $L_{FIR}/M_{H_2} = 1$ and $10 L_{\odot}/M_{\odot}$ in each plot. The WP sample galaxies, which show a marginal excess in SFE (Perea et al. 1997), also lie mainly in the same region. Therefore they all seem to share a common efficiency of converting gas into FIR luminosity. The only exception is the SP subsample which displays an enhanced SFE as already known ($L_{FIR}/M_{H_2} = 5$ to $40 L_{\odot}/M_{\odot}$ – Sanders et al. 1986; SS88; Young & Scoville 1991). Since molecular gas content is independent of interaction environment, this increase in SFE is really due to larger FIR emission. The HCG galaxies with a normal level of molecular gas content and FIR emission thus show no measurable enhancement in SFE. One exception is HCG 31ac which shows a significantly high L_{FIR}/M_{H_2} ratio of $57 L_{\odot}/M_{\odot}$, characteristic of a strongly interacting or merging starburst galaxy. This may be due to low CO luminosity (see below), but this pair is also undergoing a strong tidal interaction and a burst of star formation.

6. Discussion

6.1. Tidal Interactions and Induced Activities in Compact Group Environment

Hickson Compact Groups represent a unique environment with high galaxy density and low velocity dispersion, comparable to the cores of rich clusters such as Coma. In contrast to the cluster environment, the majority of our HCG sample consist largely of

late-type galaxies with Hubble type composition similar to the field and loose groups, and they represent the highest density environment for late-type galaxies. The main objective of this paper is to address whether frequent tidal encounters which may occur in these groups induce activities and transformations of the member galaxies.

Enhancement of CO emission and thus molecular gas content for interacting galaxies has been suggested previously in the literature, perhaps by inflow of cold gas from reservoirs outside or within (e.g. Braine & Combes 1993; Combes et al. 1994), and similar enhanced CO emission may be expected if tidal interactions are frequent among HCG galaxies. However, CO emission among the HCG spiral galaxies follow largely the same non-linear behavior derived from the samples of isolated spiral galaxies, and there is no evidence for any enhanced molecular gas content among HCG galaxies (see Figure 3). Previous reports of enhanced CO emission among interacting galaxies are likely due to the strongly non-linear $L_B - M_{H_2}$ relationship and biased sample selection towards high luminosity galaxies (Perea et al. 1997). Surprisingly, 20% of HCG spiral galaxies show *deficiency* of CO emission, and we discuss below possible causes for the reduced CO emission and molecular gas content.

Enhanced star formation and associated large FIR luminosity in gas rich spiral galaxies undergoing a tidal interaction have been well documented by both observational and numerical studies (e.g., Larson & Tinsley 1978; Bushouse 1987; SS88; Sanders et al. 1991; Surace et al. 1993; Mihos & Hernquist 1996). In the dense spiral-rich environment constituted by HCGs, we expect *a priori* an enhanced level of FIR emission if tidal encounters are frequent. On the contrary, the level of FIR emission is comparable to isolated galaxies, Virgo spirals, and weakly interacting pairs, and only strongly perturbed pairs and mergers shows clear signs of enhanced FIR emission (see §4.1 and Perea et al. 1997). An explanation may lie with the fact that only 10% of our distance limited complete sample of HCG galaxies show clear signs of strong tidal disruption such as tails and bridges, and their

similar level of FIR emission with isolated and weakly interacting samples must be then because most tidal disruptions in compact group environment are mild in nature.

This weak dependence of induced star formation on environment is likely due to highly non-linear nature of tidal disruption. In the impulse approximation of tidal disruption, the tidal acceleration experienced scales as $1/vr^2$ where v is the encounter velocity and r is the impact distance. In a cluster the encounter velocities are much larger ($v > 1000$ km s⁻¹) and the resulting tidal disruption and tidally induced activities would be 5-10 times smaller compared with an interacting pair with the same impact distance. Little or no enhancement in FIR emission among Virgo cluster spirals is consistent with this expectation. In compact group environment velocity dispersions are low, comparable to the orbital speed of interacting pairs while the galaxy density may be as high as the cores of rich clusters (Hickson et al. 1992). Therefore one may expect similar or even a higher level of tidally induced activities as in interacting pairs. The level of FIR emission among the HCG galaxies is similar to that of the isolated sample, and one may conclude that small impact distance collisions are rare in compact group environment, and even a high frequency of encounters in compact group may have relatively little impact on the overall level of induced activities.

Sulentic & Rabaça (1994) have proposed HI deficiency (Williams & Van Gorkom 1995; Huchtmeier 1997), and thus a low fuel supply for star formation, as the explanation for a level of star formation among HCG galaxies similar to the isolated sample. The HI deficiency is not likely a direct explanation since stars form in molecular gas, whose abundance is found to be mostly normal (§3.1). Jog & Solomon (1992) suggest that during direct encounters, atomic clouds collide and produce an overpressure in hot ionized gas and trigger a burst of star formation produced by a radiative shock compression of the outer layers of GMCs. For the HCG galaxies that are HI deficient, this induced star formation

process may be quenched.

A factor 2 enhancement in the I_{25}/I_{100} ratio is detected among the HCG galaxies, and we have interpreted this as HII galaxy like localized starburst, probably in the nuclear region based on the radio continuum observations by Menon (1995). The enhancement in 25 μm emission among the HCG galaxies may be the result of frequent (but weak) tidal encounters in the compact group environment.

6.2. CO Deficiency in HCG Spirals

While the majority of the HCG spiral galaxies show similar level of molecular gas content as isolated spirals, some 20% of the HCG spirals show deficiency of CO emission and presumably low molecular gas content. While the total number of CO deficient galaxies is small, a telling evidence for their special nature is that these CO deficient spirals seem to occur in specific groups (e.g. HCG 31, HCG 92) rather than randomly occurring. This deficiency may be related to the dynamical evolution of the individual groups since the prominent CO deficient groups are also the most dynamically evolved groups – as evidenced by the common HI envelopes in HCG 31 (Williams, McMahon, & van Gorkom 1991) and extended HI, stellar, and X-ray emission in HCG 92 (Shostak, Allen, & Sullivan 1984; Sulentic et al. 1995). High resolution mapping of CO emission in two CO deficient groups HCG 31 and HCG 92 using the OVRO millimeter interferometer have revealed highly disturbed molecular gas distribution in the individual galaxies (Yun et al. 1997).

Similar deficiency of HI emission among HCGs is also reported by Williams & Rood (1987) and by Huchtmeier (1997). For the HI deficiency, tidal stripping of HI disks by frequent interactions in the group environment offers a plausible explanation, but tidal stripping of molecular gas is less likely since molecular gas is usually concentrated in the

inner disks. This has been suggested to be the case for the spirals in Virgo cluster where the HI gas has been found to be stripped from the outer disk regions (Stark et al 1986) while the molecular gas content is not changed (Young et al 1989, Perea et al 1997). Gas exhaustion through star formation is a possible mechanism that may be responsible for the CO deficiency among the most strongly interacting groups. In simulating gas hydrodynamics of gas-rich mergers, Mihos & Hernquist (1996) note the difficulty of achieving very high gas density in strongly interacting systems because of fast and efficient exhaustion of gas supply by star formation. In normal disk galaxies, the re-supply of ISM is achieved through the recycled material from evolved stars and accretion of cold gas from the outer disks and halo. Among the galaxies frequently perturbed by other companions, this re-supply of cold gas may be disrupted if outer HI disks are stripped. If the observed CO deficiency is related to the dynamical evolution of compact groups while the gas-rich, spiral-dominated groups represent a dynamically younger stage still in the process of collapsing, then their ratio may indicate the relative time scales for the initial infall phase to the final rapid group evolution phase. Because of possible selection biases in the group identification as well as poor statistics on the CO deficiency, this ratio is not well constrained, but one may estimate from the observed ratio (a lower limit) that the rapid evolution phase may be at least 1/4 as long as the phase during which a group is recognized as a spiral-rich “compact group”.

Low metallicity is not likely an important reason for the low CO luminosity observed among HCG spirals since the CO deficiency is detected among relatively bright spirals in our HCG sample ($L_B > 10^{10} L_\odot$). Optically thick in nature, CO emission is a robust tracer against moderate metallicity variations as well as moderate increase in UV radiation field associated with intense star formation activity (see Wolfire, Hollenbach, & Thelens 1993 and references therein). CO molecules may suffer significant photo-dissociation in low gas column density regions such as in the starburst region in HCG 31.

6.3. Early-Type Galaxies

The nature of CO and FIR emission in early-type galaxies in HCGs is difficult to analyze since little comparison data exists in the literature. The majority of existing CO and FIR studies of early-type galaxies are mostly for unusual galaxies with bright FIR emission. There is strong evidence that the CO and FIR detected early-type galaxies in HCGs are also unusual and perhaps closely tied to their compact group environment. For example, all of the CO detected HCG elliptical galaxies in the X-ray observed groups also show associated diffuse X-ray emission, suggesting perhaps that they belong to the more evolved groups. Evidence for tidal capture from a gas-rich companion or accretion of gas-rich dwarf also exists in some cases such as in HCG 90 (see §3.2). Whether the observed frequency is any higher than the field or loose group environment is uncertain, but the presence of a number of early-type galaxies with unusual CO and FIR properties lends further support for the frequent tidal interactions in a compact group environment.

7. Summary

We have conducted a study of a distance limited complete sample of Hickson Compact Groups galaxies for CO and FIR emission in 80 and 161 galaxies, respectively and found that the CO and FIR emission in Hickson Compact Group galaxies are at a level similar to the comparison samples of isolated, Virgo cluster, and weakly interacting galaxies. About 20% of HCG spiral galaxies are deficient in CO emission, and gas exhaustion through star formation along with reduced gas reservoir through tidal stripping of the outer HI disks may offer an explanation. While the FIR emission from HCG spirals as a group is indistinguishable from the comparison samples of field and Virgo cluster spirals, some evidence for localized intense burst of star formation, probably in the circum-nuclear regions, is found in the enhancement of I_{25}/I_{100} ratios. Some groups such as HCG 31 or

HCG 92 may be well advanced in their evolutions if their CO deficiency is dynamical in nature. Along with the CO and HI deficiency in some of the HCGs, presence of early-type galaxies with significant CO and FIR emission lends a further support to frequent tidal interaction and accretion events in compact group environment.

The authors thank the staff of the NRAO 12-m telescope and the Haystack observatory for their assistance with the observations. We also thank D. Benford and J. Girart with the CO observations at the CSO and Haystack observatory. LVM acknowledges financial support and hospitality from the Harvard-Smithsonian Center for Astrophysics (USA). JP, AO and LV-M are partially supported by DGICYT (Spain) Grant PB93-0159 and PB6-0921 and Junta de Andalucía (Spain). MSY is supported by the NRAO Jansky Research Fellowship.

A. SCANPI Statistics on Radio-Loud QSOs

The positional accuracy and possible source confusion as well as the calibration of the IRAS SCANPI data are tested by analyzing the data on radio-loud QSOs. A list of candidate QSOs with IRAS detection was compiled from the literature (Neugebauer et al. 1986) and from our own search (in collaboration with L. Armus). This list is further reduced to 29 objects by requiring that they are radio-loud objects and a VLA calibrator – this extra step ensures having highly accurate coordinate information on each source. SCANPI data are obtained and analyzed in the same manner as for the HCG sample (see §2.3), and 27 out of 29 objects in the list are detected with S/N of 3 or better at 60 μm (Table A-1). Both for this analysis and in the source identification for the HCG sample, 60 μm band is used because of its superior sensitivity over the other bands, both in raw sensitivity and favorable spectral energy distribution among these extragalactic sources.

The calibration of the SCANPI data is checked by comparing the measured flux against the pointed observations by Neugebauer et al. and is shown in Figure A-1. In general published and new SCANPI fluxes agree well with a few exceptions. There are four objects (out of 19 plotted) that show significant disagreement. While measurement inconsistencies are possible, a likely explanation is that many of these sources are known BL Lac or optical variables whose observed flux may fluctuate by a factor of a few in several months time scale, and the observed disagreement is well within this intrinsic variability. Therefore, the calibration of SCANPI data appears reliable.

The “miss” parameter given by the SCANPI processor is the offset in the source position along the average scan direction with respect to the specified source position, and this parameter is used as the primary measure of source identification. A histogram of the miss parameter for the 27 detected QSO sample is shown in Figure A-2. While the majority of the points lie clustered around the zero offset, two objects are detected with a miss

parameter larger than $20''$. A source confusion is suspected for these two, and Digitized Sky Survey plates are examined for all detected sources. As summarized in Table A-1, potential source confusion exists for several objects, and the two highly discrepant objects appear indeed due to source confusion and/or low S/N in the measurements. Excluding these two objects, the standard deviation of “miss” parameter for the remaining 25 objects is $6''.7$ – about 1/10 of the intrinsic spatial resolution, which is reasonably expected. The determination of source centroid depends somewhat on the S/N of the measurement, and the standard deviation for the 18 objects with $S/N > 5$ decreases to $5''.5$.

For the analysis of the HCG sample, we assume that the statistics obtained from the QSO sample generally apply, including both the intrinsic scatter and the source confusion. One major concern in this assumption is the interplay between the S/N and the position determination. The range of S/N for both the radio QSO and HCG sample are summarized in Table A-2. Over one half (37) of all HCG galaxies are detected with $S/N > 20$, and the source identification along the average scan direction should be excellent for the HCG sample. For the remaining 35 galaxies, the S/N distribution for detection is similar to that of the QSO sample. Therefore, the standard deviation derived from the analysis of the QSO sample may be safely taken as the upper limit of error in the source identification in the HCG sample.

REFERENCES

- Allam, S., Assendorp, R., Longo, G., Braun, M., & Richter, G. 1996, *A&AS*, 117, 39
- Bettoni, D. & Fasano, G. 1993, *AJ*, 1291, 105
- Boselli, A., Casoli, F., Lequeux, J. 1995, *A&A*, 110, 521
- Boselli, A., Mendes de Oliveira, C., Balkowski, C., Cayatte, V., Casoli, F. 1996, *A&A*, 314, 738
- Bothum, G. D., Lonsdale, C. J., Rice, W. 1989, *ApJ*, 341, 129
- Braine, J., & Combes, F. 1993, *A&AS*, 97, 887
- Burstein, D., & Heiles, C. 1984, *ApJS*, 54, 33
- Bushouse, H. A. 1987, *ApJ*, 320, 49
- Combes, F., Prugniel, P., Rampazzo, R., Sulentic, J. W. 1994, *A&A* 281, 725
- de Vaucouleurs, G., de Vaucouleurs, A., Corwin, H. G., Buta, R. J., Paturel, G., Fouqué, P. 1991, *Third Reference Catalogue of Bright Galaxies*, Springer, Berlin (RC3)
- Dultzin-Hacyan, D., Moles, M., & Masegosa, J. 1988, *A&A*, 206, 95
- Dultzin-Hacyan, D., Masegosa, J. & Moles, M. 1990, *A&A*, 238, 28
- Fasano, G. & Bettoni, D. 1994, *AJ*, 107, 1649
- Feigelson, E. D., & Nelson, P. I. 1985, *ApJ*, 293, 192
- Heckman, T. M., Blitz, L., Wilson, A. S., Armus, L. & Miley, G. K. 1989, *ApJ*, 342, 735
- Helou, G., Khan, I.R., Malek, L., & Boehmer, L. 1988, *ApJS*, 68, 151.

- Hickson, P. 1982, ApJ, 255, 382
- Hickson, P. 1993, ApLett&Comm, 29, 1
- Hickson, P., Menon, T. K., Palumbo, G. G. C., & Persic, M. 1989b, ApJ, 341,679 (HMPP)
- Hickson, P., Kindl, E., & Auman, J. R. 1989a, ApJS, 70,687 (HKA)
- Hickson, P., Mendes de Oliveira, C., Huchra, J. P., Palumbo, G. G. C., 1992, ApJ, 399, 353.
- Huchtmeier, W. K., & Tammann, G. A. 1992, A&A, 257, 455
- Huchtmeier, W. K. 1997, A&A, in press
- Hummel, E., Van der Hulst, J. M., Kennicutt, R. C. & Keel, W. C. 1990, A&A, 236, 333
- Hummel, E. 1981, A&A, 96, 111
- Isobe, T., & Feigelson, E. D. 1990, BAAS, 22, 917
- Isobe, T., Feigelson, E. D., & Nelson, P. I. 1986, ApJ, 306, 490
- Jog, Ch. J., & Solomon, P. M. 1992, ApJ, 387, 152
- Karachentseva, V.E., Lebedev, V.S., & Shcherbanovskij, A.L. 1973, Comm. of Special
Astrophys. Obs. USSR 8
- Kenney, J. D., & Young, J. S. 1988a, ApJS, 66, 261
- Kenney, J. D., & Young, J. S. 1988b, ApJS, 326, 588
- LaValley, M., Isobe, T. & Feigelson, E.D. “ASURV”, 1992, BAAS, in The new software
report for ASURV Rev. 1.1.
- Larson, R.B. & Tinsley, B.M. 1978, ApJ, 219, 46

- Lees, J. F., Knapp, G. R., Rupen, M. & Phillips, T. G. 1991, *ApJ*, 379, 177
- Longo, G. Busarello, G., Lorenz, H. Richter, G. and Zagiia, S. 1994, *A&A*, 282, 418
- Marston, A. P. 1988, *MNRAS*, 231, 333
- Menon, T. K. 1995, *MNRAS*, 274, 845
- Menon, T. K., & Hickson, P. 1985, *ApJ*, 296, 60
- Mihos, J. C., & Hernquist, L. 1996, *ApJ*, 464, 641
- Moles, M., del Olmo A., Perea J., Masegosa J, Márquez I. & Costa V. 1994, *A&A*, 285, 404.
- Neugebauer, G., Soifer, B. T., Miley, G. K., Clegg, P. E., 1986, *ApJ*, 308, 815
- Perea, J., Del Olmo, A., Verdes-Montenegro, L., & Yun, M. S. 1997, *ApJ*, in press
- Rubin, V. C., Hunter, D. A., & Ford, W. K., 1991, *ApJS*, 76, 153
- Sage, L. J. 1993, *A&A*, 272, 123
- Sanders, D. B., Scoville, N. Z., & Soifer, B. T. 1991, *ApJ*, 370, 158
- Sanders, D. B., Scoville, N. Z., Young, J. S., Soifer, B. T., Schloerb, F. P., Rice, W. L.,
Danielson, G. E. 1986, *ApJ*, 305, L45
- Savage, B. D., & Mathis, J. S. 1979 *ARA&A*, 17, 73
- Shostak, G. S., Allen, R. J., & Sullivan, W. T., III, 1984, *A & A*, 139, 15
- Solomon, P. M., & Sage, L. J. 1988, *ApJ*, 334, 613 (SS88)
- Stark, A. A., Knapp, G. R., Bally, J., Wilson, R. W., Penzias, A. A., & Rowe, H. B. 1986,
ApJ 310, 660

- Sulentic, J. W., Pietsch, W., & Arp, H., 1995, *A & A*, 298, 420
- Sulentic J. W. & de Mello Rabaça D. F. 1993, *ApJ*, 410, 520.
- Sulentic J. W. & Rabaça C. R. 1994, *ApJ*, 429, 531.
- Surace, J. A., Mazzarella, J., Soifer, B. T., Wehrle, A. E. 1993, *AJ*, 105, 864
- Tully, R. B. 1988, *Nearby Galaxies Catalog*, Cambridge ; New York : Cambridge University Press
- Venugopal, V. R. 1995, *MNRAS*, 277, 455
- Verdes-Montenegro, L., del Olmo, A., Perea, J., Athanassoula, E., Márquez, I., & Augarde, R. 1997, *A&A*, 321, 409
- Wiklind, T., Combes, F., Henkel, C. 1995, *A&A*, 297, 643
- Williams, B. A. & Rood, H. J. 1987, *ApJS*, 63, 265
- Williams, B. A., McMahon, P. M., & van Gorkom, J. H., 1991, *AJ*, 101, 1957
- Williams, B. A., & Van Gorkom, J. H. 1995 in *Groups of galaxies*, ed. O. G. Richter & K. Borne, ASP Conference Series, Vol. 70, 77
- Wolfire, M. G., Hollenbach, D., & Tielens, A. G. G. 1993, *ApJ*, 402, 195
- Xu., C. & Sulentic, J.W. 1991, *ApJ*, 374, 467
- Young, J. S., & Scoville, N. Z. 1991, *ARA&A*, 29, 581
- Young, J. S. et al. 1995, *ApJS*, 98, 219
- Young, J. S., Xie, S., Keney, J. D., & Rice, W. L. 1989, *ApJS* 70, 699
- Yun, M.S., Verdes-Montenegro, L., del Olmo, A. & Perea, J. 1997, *ApJ*, 475, L21

Zepf, S. E., Whitmore, B. C. & Levison, H. F. 1991, ApJ, 383, 524

Fig. 1.— The CO spectra of the 21 galaxies and 3 unresolved pairs that are detected. Five galaxies from our HCG sample have been detected by other authors (H7a and all four members of HCG 16 by Boselli et al 1996) and are not shown here. The optical velocities of each galaxy are marked with an arrow. The CO spectra of IC 883, NGC 2738, and NGC 6090, observed for system tests are also shown.

Fig. 2.— (a) Cumulative blue luminosity functions for the 80 HCG galaxies observed in CO from our distance limited sample and the comparison sample galaxies. (b) Cumulative blue luminosity functions for the 161 HCG galaxies analyzed with ADDSCAN/SCANPI and 212 galaxies of the CIG comparison sample of isolated galaxies. The HCG and CIG samples have similar luminosity distribution, but the isolated and Virgo cluster samples lack bright galaxies. The WP and SP samples include proportionally more luminous galaxies.

Fig. 3.— The dependence of L_B on M_{H_2} for (a) HCG galaxies and (b) interacting galaxies belonging to the VC, WP and SP samples. The solid line corresponds to the best fit model for the isolated galaxies, $\log L_B = (0.57 \pm 0.03) \log M_{H_2} + (4.9 \pm 0.6)$ (see Perea et al. 1997). Large symbols in HCGs data correspond to late-type galaxies while small symbols correspond to early-type galaxies. Open triangles are upper limits in H_2 . The crossed circles correspond to the summed values for the unresolved pairs H31ac, H38bc and H90bd. The dotted line marks the range of M_{H_2} of H31b from the single dish observations (upper limit) and the OVRO data (lower limit; Yun et al. 1997).

Fig. 4.— Histograms of the residuals $\Delta[\log(M_{H_2})]$ relative to the power law template of isolated galaxies (dashed line) and all HCGs spiral galaxies (solid line). The distribution of residuals for the HCG spiral is skewed, and the comparison with the CIG sample suggests that 20% of the HCG spirals are deficient in molecular gas content (by a factor ≥ 10).

Fig. 5.— The dependence of L_B on L_{FIR} for (a) CIG sample, (b) SP sample, (c) all HCG

galaxies, and (d) HCG spirals only. The solid line corresponds to the power law best describing the CIG sample. Open triangles are upper limits in FIR. Encircled points are the unresolved pairs with summed values. In comparison, only the SP sample shows significant FIR excess from the template relation derived from the isolated galaxy sample.

Fig. 6.— Histograms of the residuals $\Delta[\log(L_{FIR})]$ relative to the power law derived from the CIG sample (dashed line). The solid lines correspond to (a) all HCGs spiral galaxies and (b) only HCGs spirals detected at both $60\mu\text{m}$ and $100\mu\text{m}$ bands. The broader distribution of residuals for the HCG spirals is in part due to larger associated measurement uncertainties, but it may also reflect real physical effect. When only the detected objects are considered (Fig. 6b), an impression of an apparent FIR enhancement may be deduced, and all upper limits should be included in this analysis.

Fig. 7.— Histogram of $\log(I_{25}/I_{100})$ for (a) CIG sample (dotted line) and HCGs galaxies (solid line) and (b) starburst and HII galaxies from Dultzin-Hacyan et al. (1990; dashed line).

Fig. 8.— Cumulative luminosity distributions for the HCG spiral and CIG samples at (a) $25\mu\text{m}$ and (b) $100\mu\text{m}$. While the $100\mu\text{m}$ distribution is similar for the two samples, there is a clear enhancement in $25\mu\text{m}$ emission among the HCG sample.

Fig. 9.— Dependence of L_{FIR} on M_{H_2} for HCG galaxies and three interacting comparison samples. The plotted lines correspond to the ratios $L_{FIR}/M_{H_2} = 1, 10$ and $100 L_{\odot}/M_{\odot}$ – a measure of efficiency converting gas to luminosity (e.g., Sanders et al. 1991). The dots in the HCGs plot are upper limits in both axis, and open triangles are upper limits. The small dotted line corresponds to the range of M_{H_2} for H31b from the single dish observations (upper limit) and the OVRO data (lower limit; Yun et al (1997)).

Fig. A-1.— Comparison of IRAS $60\mu\text{m}$ fluxes for the 19 radio-loud QSO's reported by

Neugebauer et al. (1986) and the XSCANPI data. The agreement is rather good except for a few objects, and the difference can be accounted by intrinsic variability of these QSO's.

Fig. A-2.— Histogram of “miss” parameters for the 27 detected QSO's. Excluding the two outlying sources, which are likely due to source confusion, the standard deviation of miss parameter is $6.7''$ for the entire sample and $5.5''$ for the 18 objects detected with $S/N > 5$ (shaded area).